@AstroOrca

LIGO SEMINAR

MULTI-DETECTOR NETWORK DETECTION AND CHARACTERISATION OF GRAVITATIONAL-WAVE BURSTS WITH THE *BAYESWAVE* PIPELINE

29TH OF MARCH 2024

YI SHUEN (CHRISTINE) LEE

PROF. ANDREW MELATOS

DR. MEG MILLHOUSE

OzGrav

ARC Centre of Excellence for Gravitational Wave Discovery

LIGO VIRGO KAGRA

THE UNIVERSITY OF MELBOURNE

TALK OVERVIEW

- Gravitational-wave (GW) bursts and Instrumental glitches
- *BayesWave* algorithm overview
- Multi-detector network analyses with *BayesWave*
  - **PART I:** Impact of noise transients on GW burst detection efficiency
  - **PART II:** Characterization of gravitational-wave burst polarizations

TYPES OF GW SOURCES

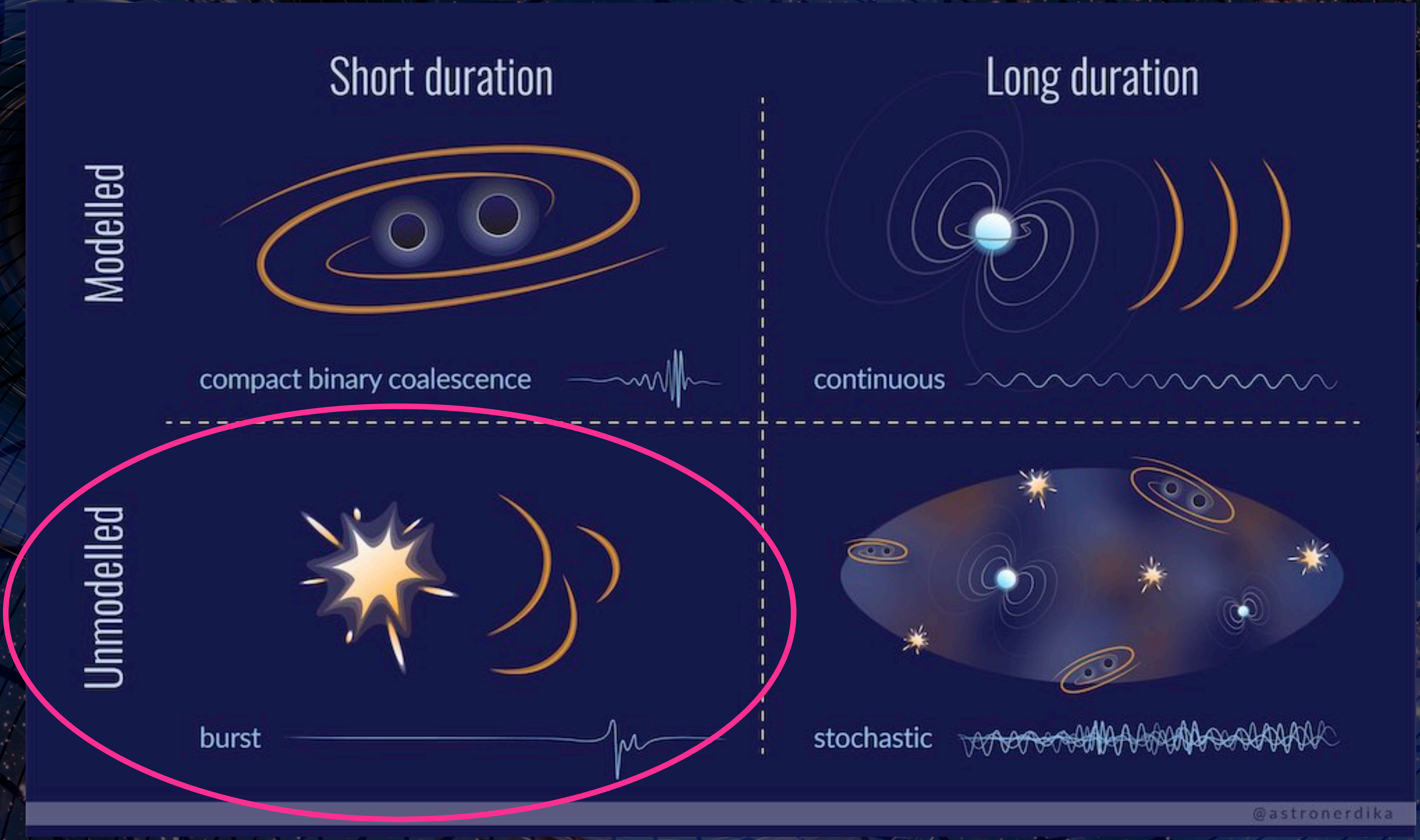

[Image credits: Shanika Galaudage]

WHY SEARCH FOR "UNMODELLED" BURSTS?

- Detection of known potential sources
  - Supernovae (SNe)
  - Gamma-ray Bursts (GRB)
- New discoveries!
  - We may not know the source, but we know what the waveform looks like

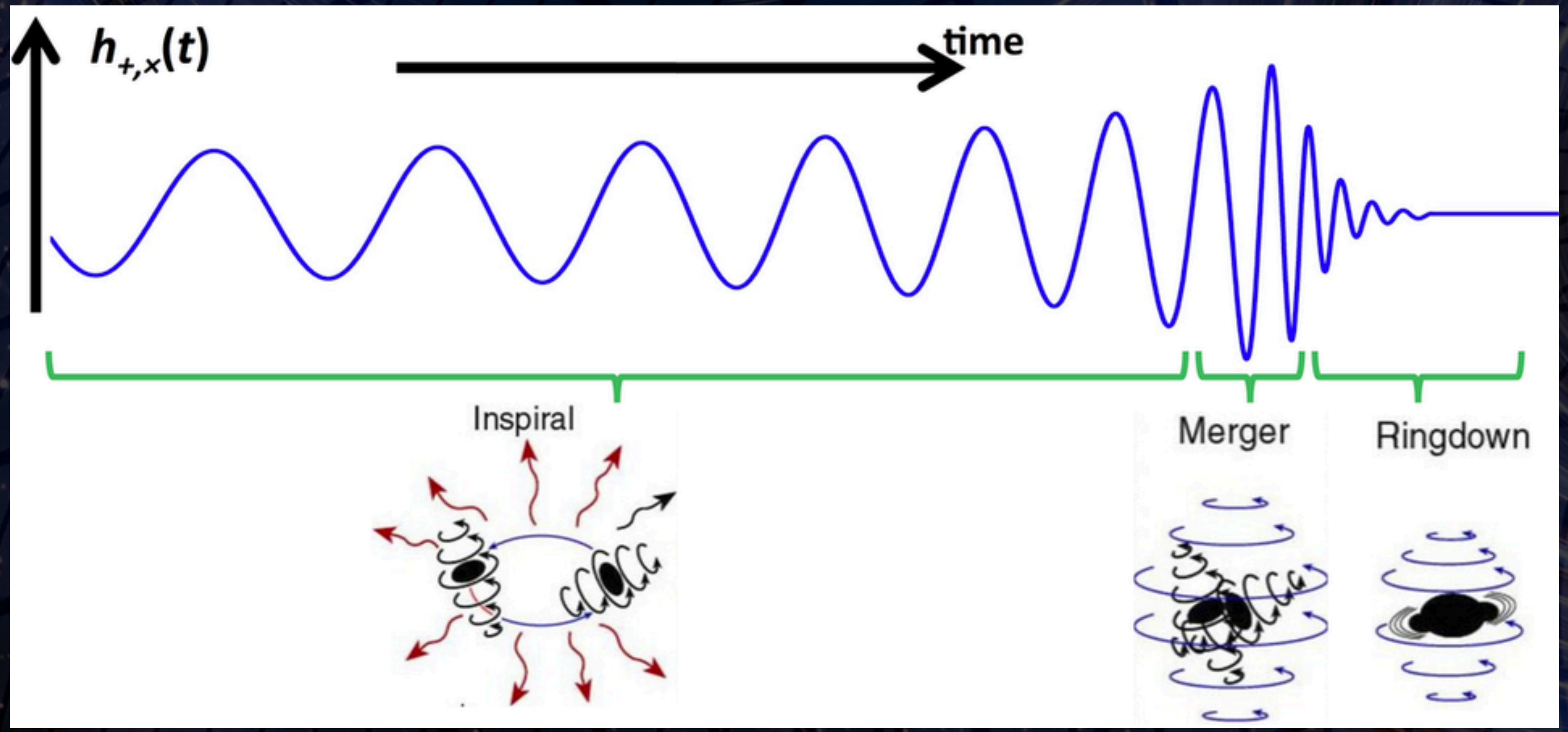

[Image: M. Favata/SXS/K. Thorne]

Modelled, well-understood waveforms (CBC)

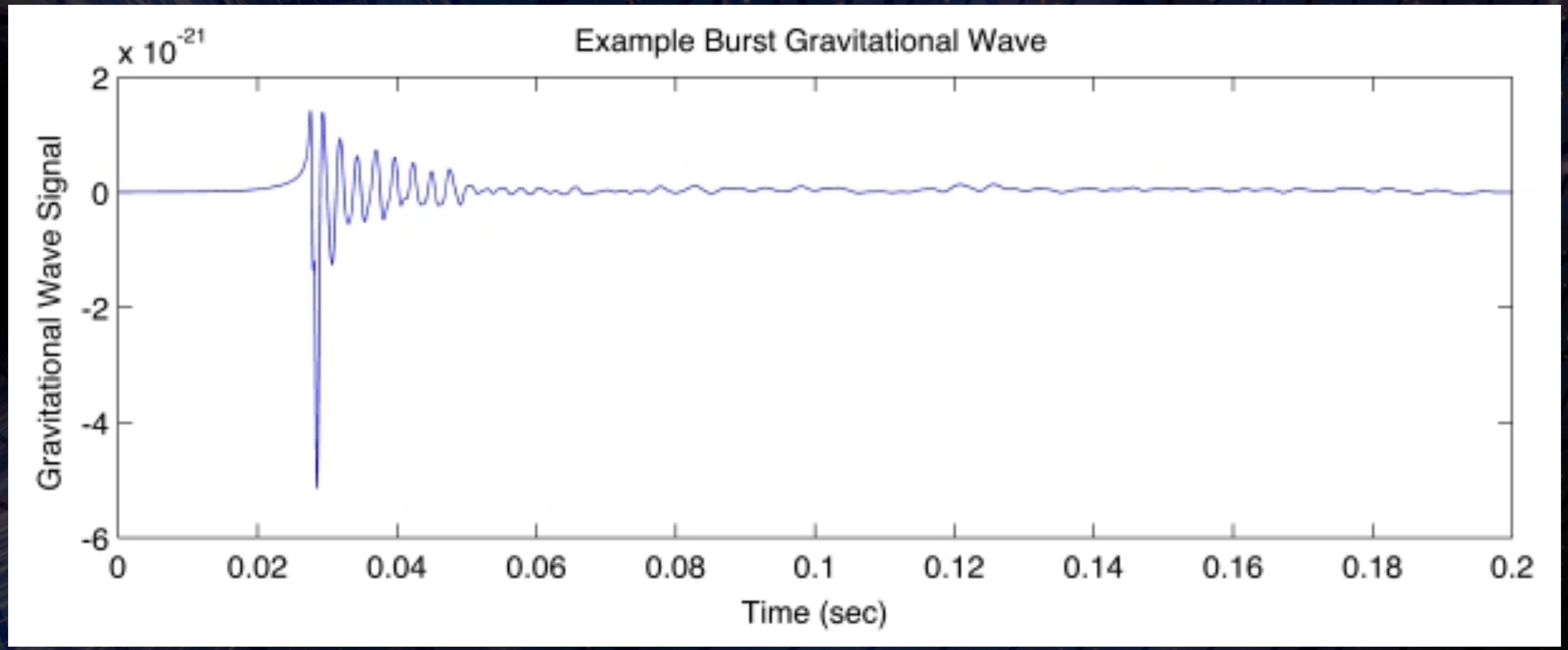

[Image: A. Stuver/LIGO using data from C. Ott, D. Burrows, et al.]

Sample unmodeled GW burst waveform

WHAT IS IN THE DETECTOR DATA?

Data = Signal (maybe) + Noise

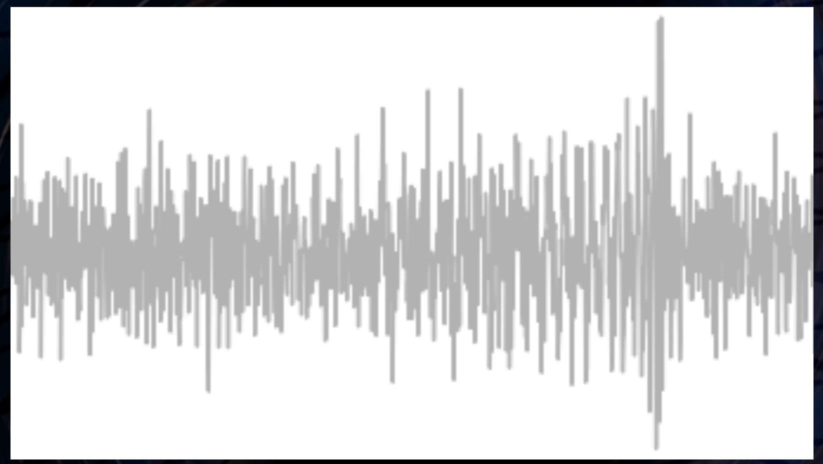

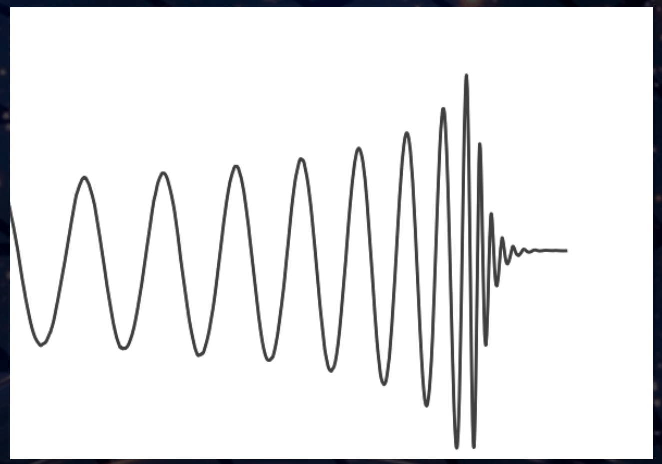

$\vec{s}$ $\qquad h(\vec{\theta})$ $\qquad \vec{n}$

Noise components:

$$\vec{n} = \overrightarrow{n_G} + \vec{g}$$

Stationary, Gaussian noise

Instrumental glitches (non-stationary, non-Gaussian)

[Adapted from Meg Millhouse's slide]

THE PROBLEM: *INSTRUMENTAL GLITCHES*

Non-astrophysical and non-Gaussian power spikes in the detector

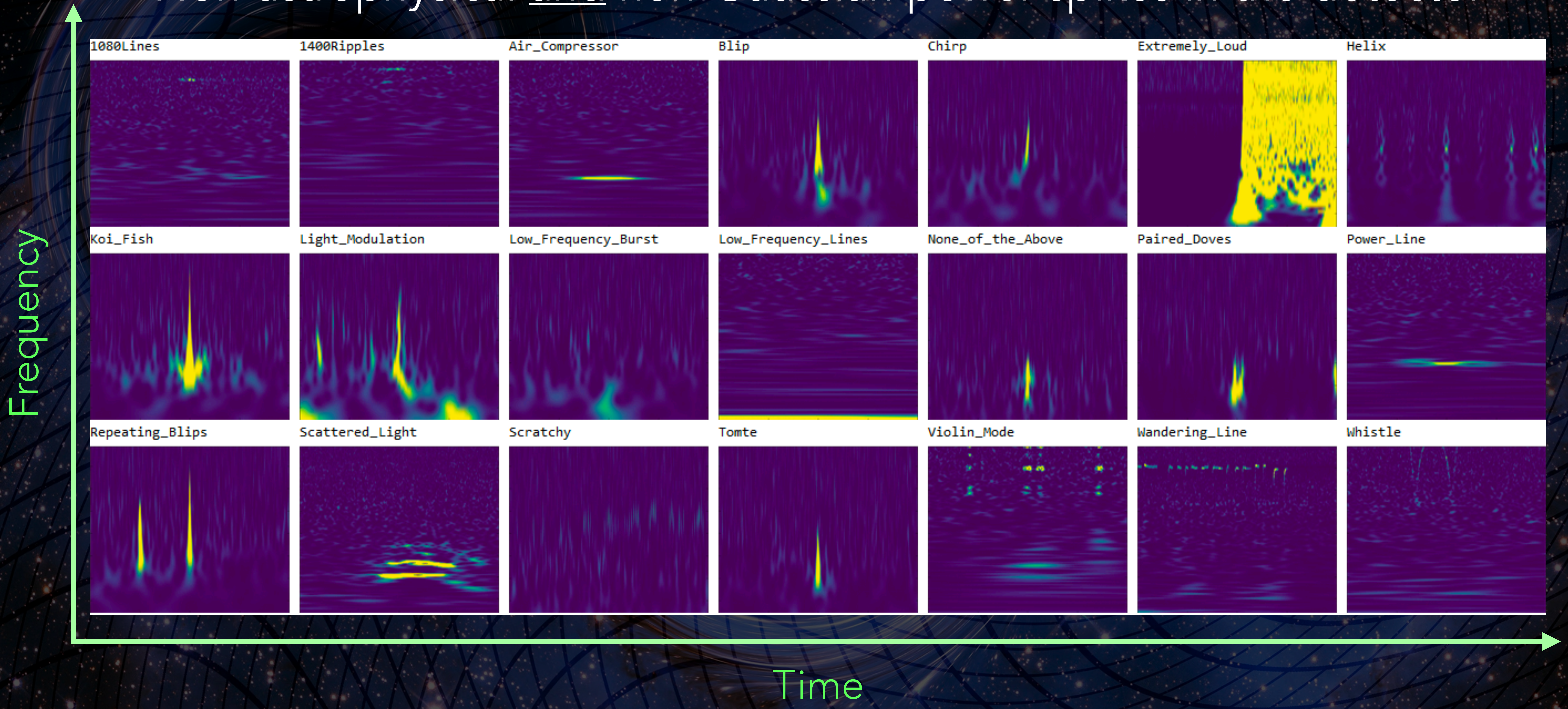

[Image from Gravity Spy]

INTRODUCING…

THE *BAYESWAVE* ALGORITHM

BAYESWAVE: *ALGORITHM OVERVIEW*

- An unmodelled transient gravitational wave (burst) analysis algorithm
- Enables joint characterization of instrumental glitches <u>and</u> GW bursts
- Reconstructs transient, non-Gaussian features in the data by summing a set of <u>sine-Gaussian wavelets</u>, with no *a priori* assumptions

Images courtesy of Meg Millhouse

<u>*BayesWave* publications:</u>
Cornish + Littenberg, Class. Quant. Grav 32, 130512 (2015)
Cornish et al., Phys. Rev. D 103, 044006 (2021)

BAYESWAVE: MODEL PARAMETERS - RJMCMC

- BayesWave uses the trans-dimensional Reversible Jump Markov Chain Monte Carlo (RJMCMC)

  1. To sample model (i.e. wavelet) parameters
  2. To sample model dimensions i.e. number of wavelets used to describe instrumental glitches and/or GW signals

- Trans-dimensional steps involve adding/removing a wavelet

RJMCMC: FINDING THE BEST FIT MODEL

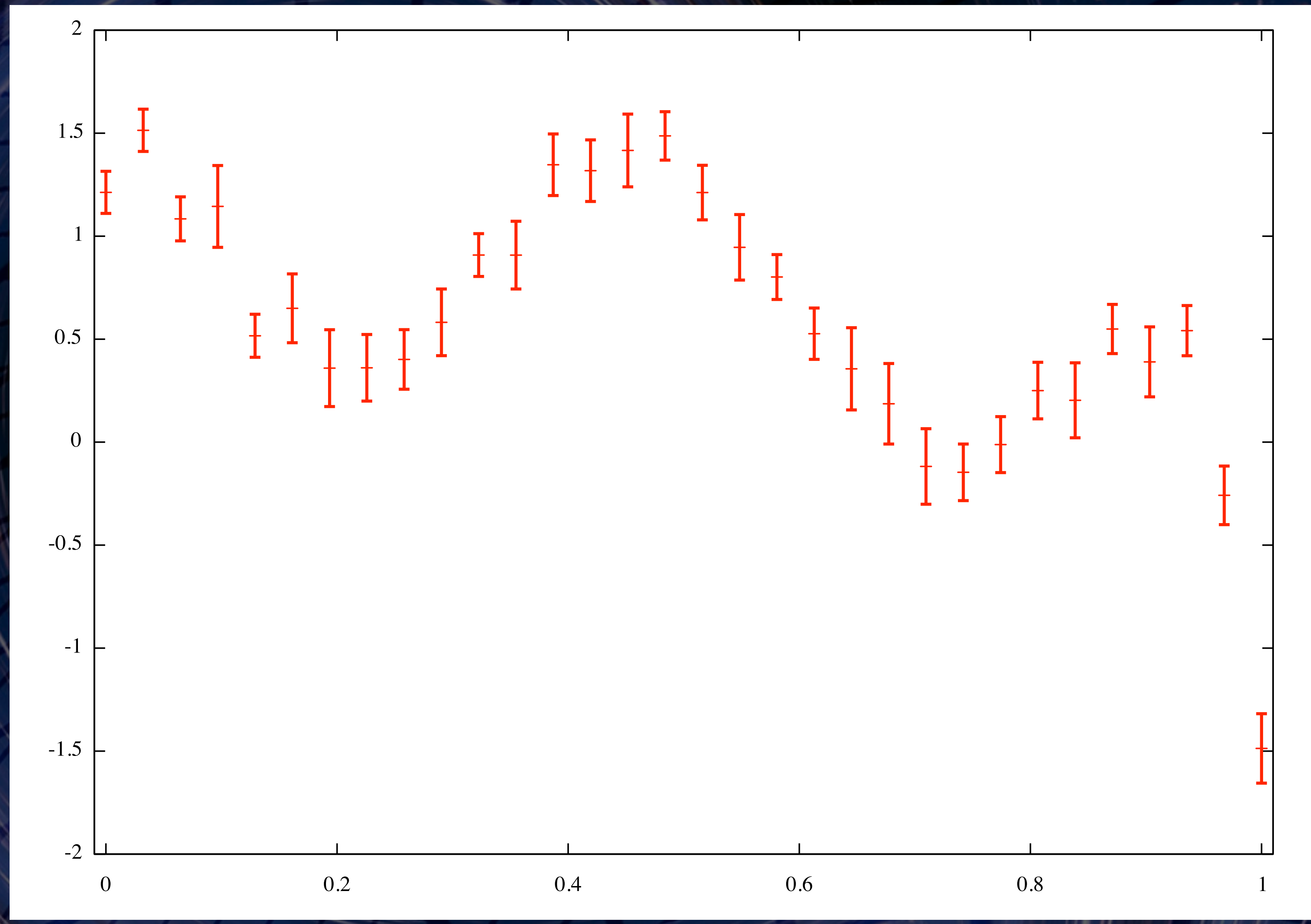

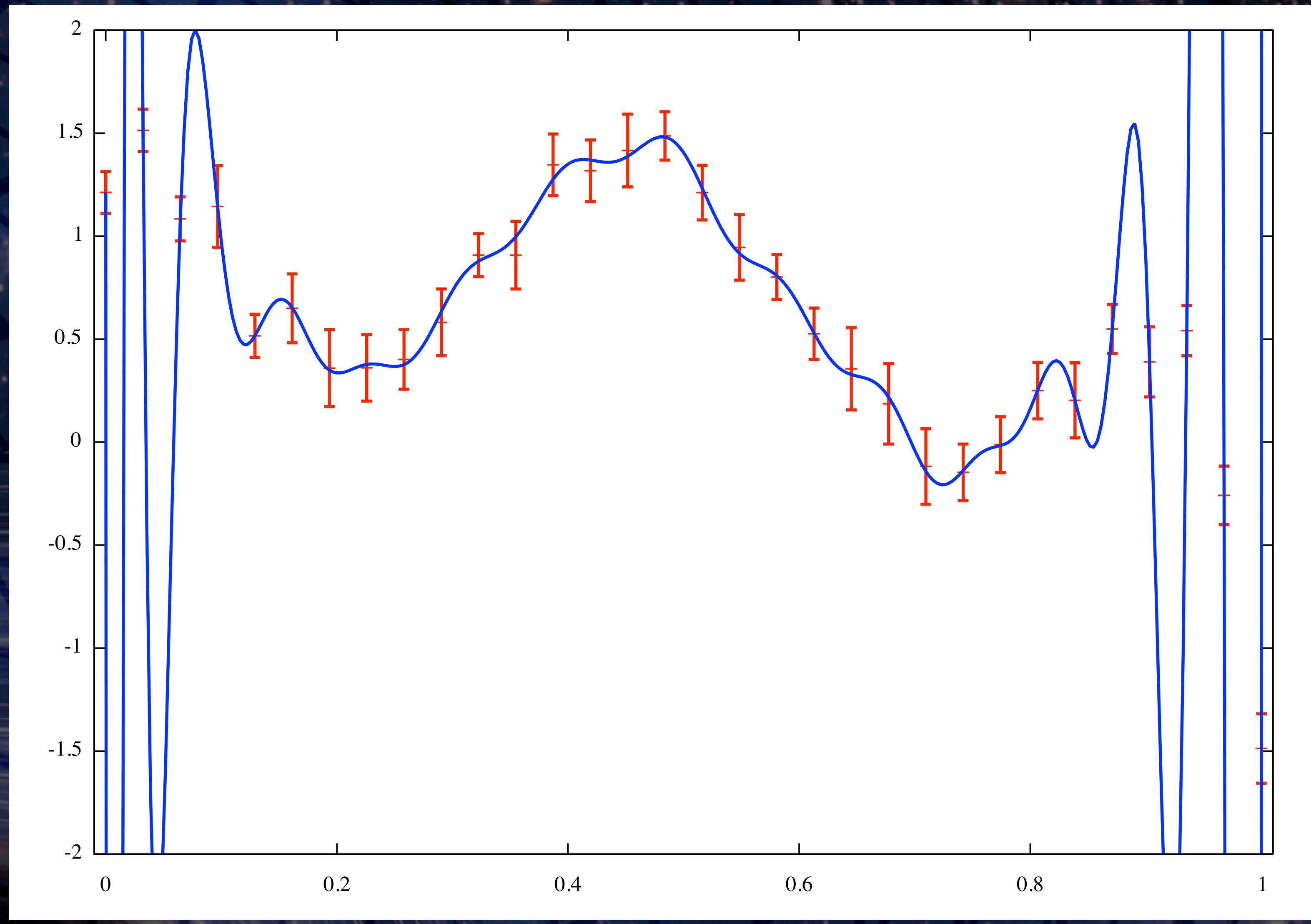

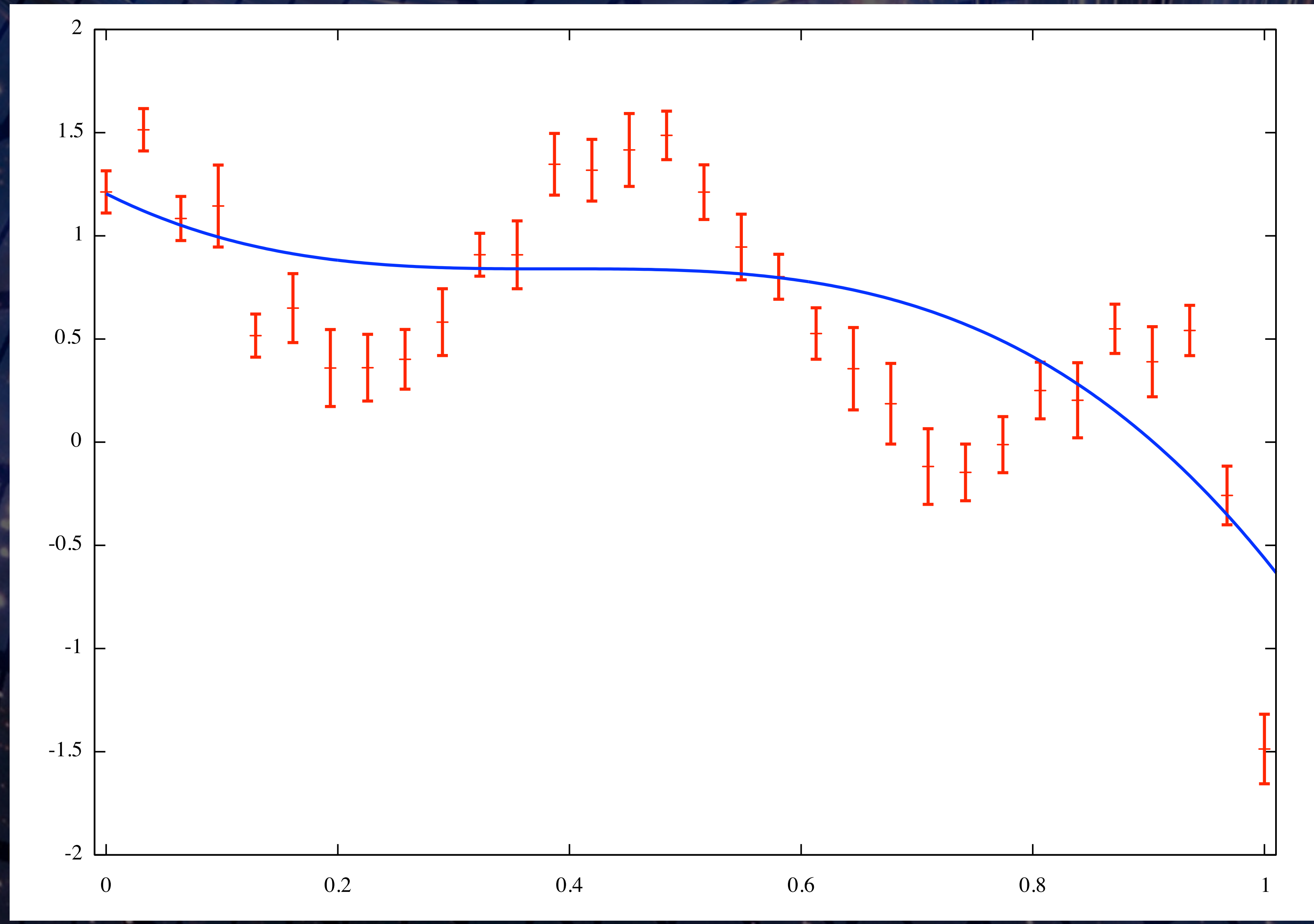

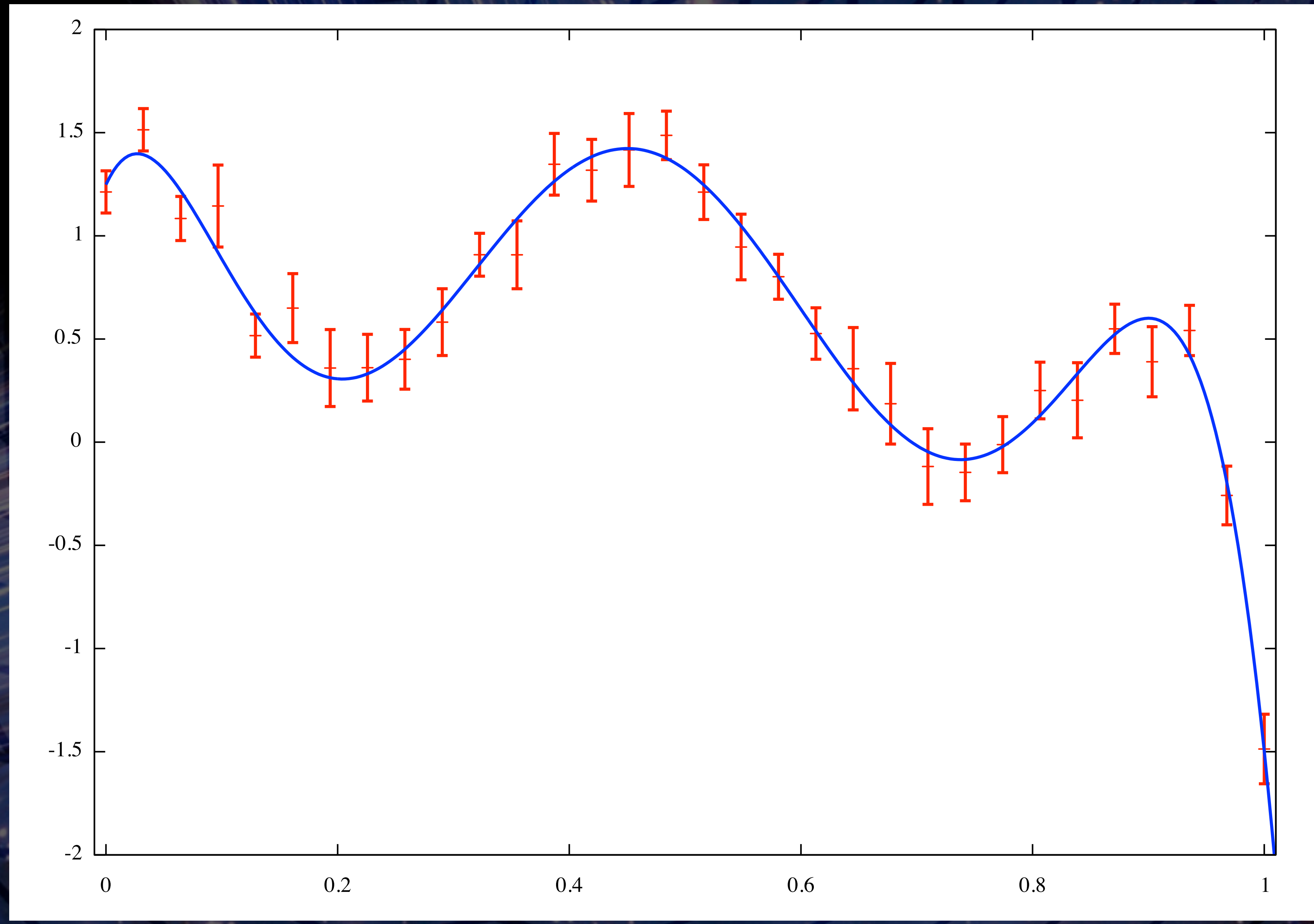

X

[Image credits: Neil Cornish]

RJMCMC:
POSTERIOR DISTRIBUTION OF SUITABLE FITS

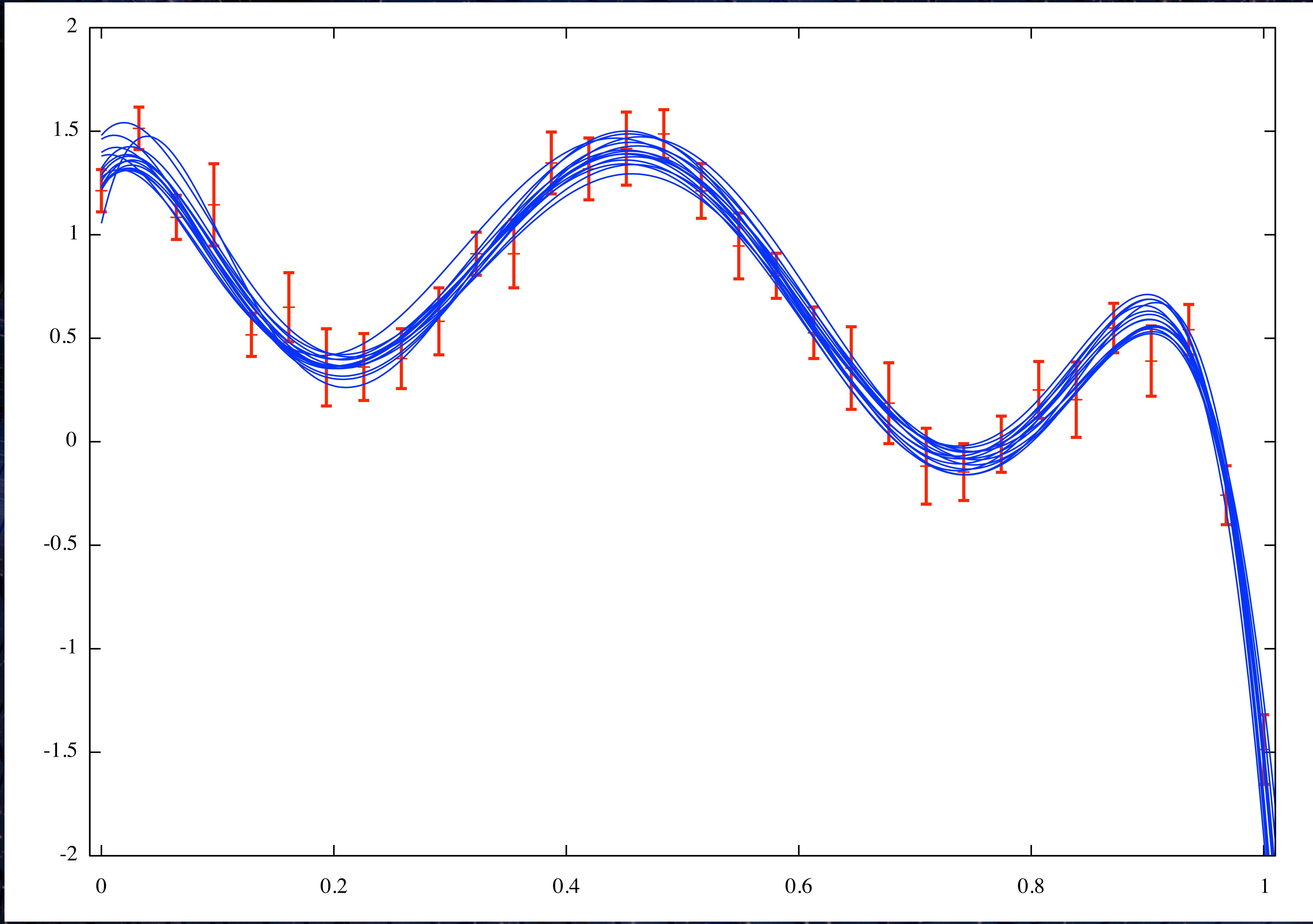

X

[Image credits: Neil Cornish]

BAYESWAVE: WAVEFORM POSTERIOR

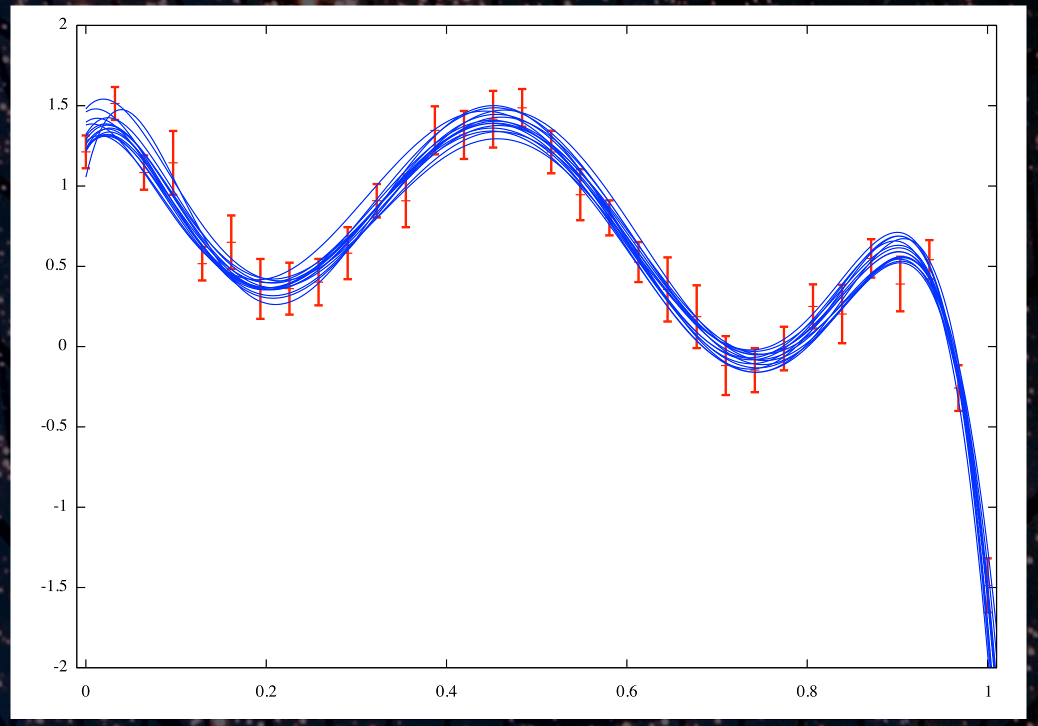

- At each MCMC iteration, we get:
  - (i) Number of wavelets, *N*
  - (ii) Parameters of each of the *N* wavelets

  from which we can construct waveform model by summing all the *N* wavelets
- **Waveform Posterior:**

  Combine waveform models across all iterations

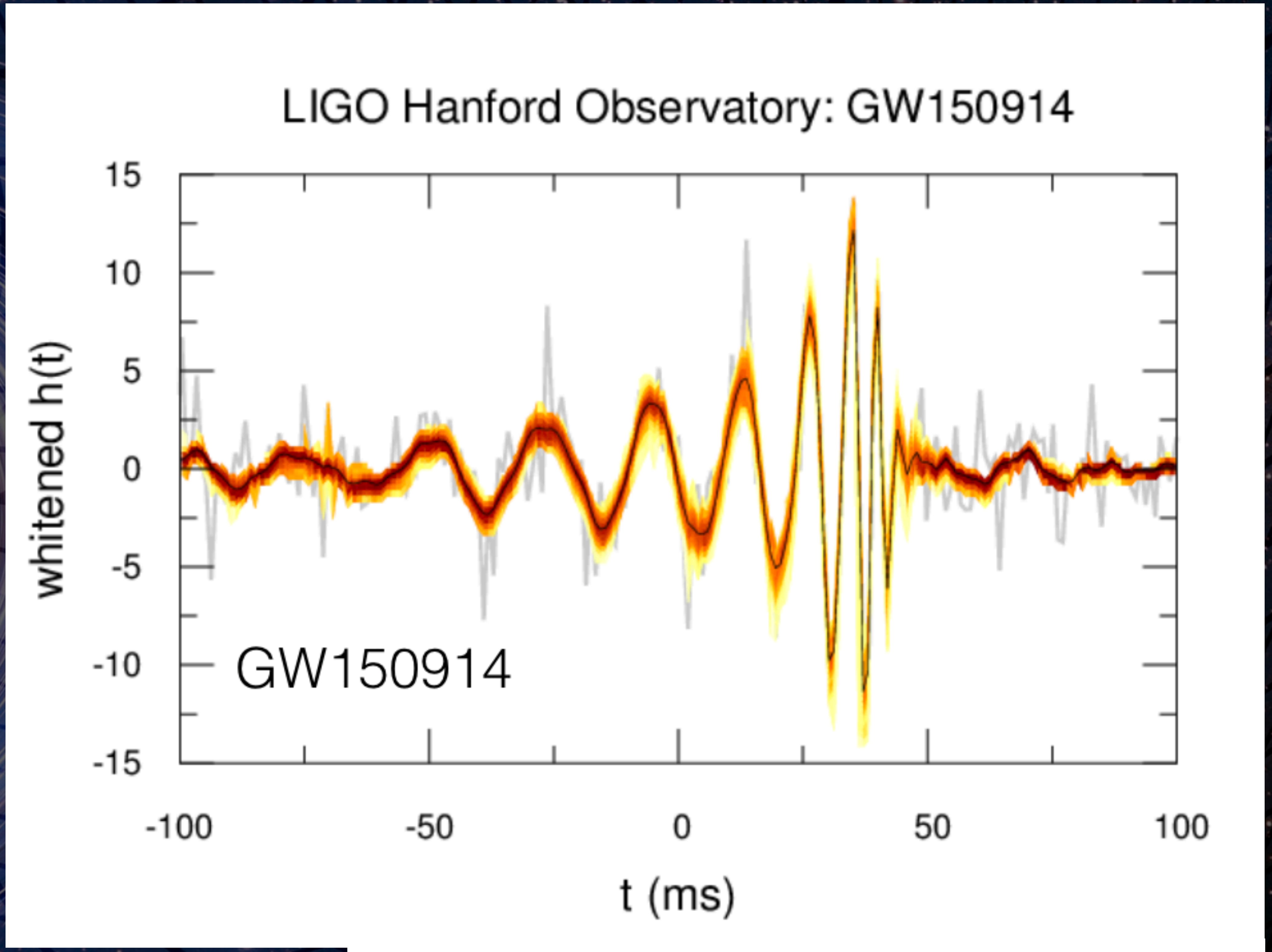

[Image courtesy of Jonah Kanner, Tyson Littenberg, and Meg Millhouse]

X

BAYESWAVE: MODEL SELECTION

- Reconstructs transient features using three independent models:
  - Signal plus Gaussian-noise model, $\mathscr{S}$
  - Glitch plus Gaussian-noise model, $\mathscr{G}$
  - Gaussian-noise only model, $\mathscr{N}$
- "Model everything and let the data sort it out"

BAYES FACTOR = Bayesian evidence ratio between two models

$$\text{e.g. } \mathscr{B}_{\mathscr{S},\mathscr{G}} = \frac{p(\vec{s}\,|\,\mathscr{S})}{p(\vec{s}\,|\,\mathscr{G})}$$

If $\ln \mathscr{B}_{\mathscr{S},\mathscr{G}} > 0 \Rightarrow\ \mathscr{S}$ is more strongly supported by data than $\mathscr{G}$

BAYESWAVE: ROLE IN GW BURST SEARCHES

- Used to follow-up searches for GW events in O1, O2 and O3 *
  To assess consistency with matched-filter (model-based) searches
- Also used to follow-up trigger events found by coherent WaveBurst (cWB) to increase detection confidence

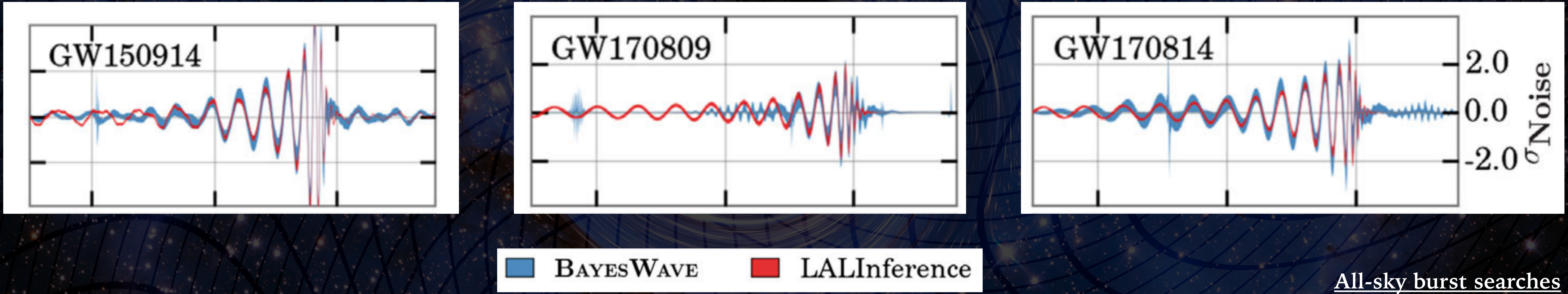

GWTC-1: Phys. Rev. X 9, 031040 (2019),
GWTC-2: Phys. Rev. X 11, 021053 (2021),
GWTC-3: arXiv:2111.03606 (2021).

<u>All-sky burst searches</u>
O1: Phys. Rev. D 95, 042003 (2017)
O2: Phys. Rev. D 100, 024017 (2019)
O3: Phys. Rev. D 104, 122004 (2021)

PART IA:

BURST DETECTION CONFIDENCE
OF *BAYESWAVE*
WITH MULTI-DETECTOR NETWORKS

Lee et al., Phys. Rev. D **103**, 062002 (2021)

EXPANDING GW DETECTOR NETWORK

- **Existing 2nd-generation ground-based detectors:**
  - (1) LIGO - Hanford and Livingston, United States
  - (2) Virgo, Italy
  - (3) KAGRA, Japan
- LIGO India approved and under commission
- Three observing runs O1, O2, O3; and O4 is happening right now

[Image credits: LIGO Lab Caltech]

ANALYTIC SCALING OF $\ln \mathscr{B}_{\mathcal{S},\mathcal{G}}$

- *BayesWave's* detection confidence quantified using the log signal-versus-glitch-model Bayes factor, $\ln \mathscr{B}_{\mathcal{S},\mathcal{G}}$

- Analytic approximation of $\ln \mathscr{B}_{\mathcal{S},\mathcal{G}}$ for a 2-detector network is

$$\ln \mathscr{B}_{\mathcal{S},\mathcal{G}} \simeq \frac{5N}{2} + N \ln V_\lambda + \boxed{5N \ln\left(\frac{\mathrm{SNR}_{\mathrm{net}}}{\sqrt{N}}\right)} - \sum_{n=1}^{N} \ln \overline{Q}_n + \left[2 + \ln \frac{\sqrt{\det C_\Omega}}{4\pi^2}\right]$$

- Main scaling: $\ln \mathscr{B}_{\mathcal{S},\mathcal{G}} \sim N \ln \mathrm{SNR}_{\mathrm{net}}$
  - (i) N : number of wavelets (i.e. model complexity)
  - (ii) $\mathrm{SNR}_{\mathrm{net}}$: signal-to-noise ratio

Littenberg et al., Phys. Rev. D, 94, 044050 (2016)

ANALYTIC SCALING OF $\ln \mathscr{B}_{\mathcal{S},\mathcal{G}}$

- Generalizing for an $\mathscr{I}$-detector network:

$$\ln \mathscr{B}_{\mathcal{S},\mathcal{G}} \simeq \boxed{(\mathscr{I}-1)}\left[\frac{5N}{2} + N\ln(V_\lambda) - \sum_{n=1}^{N} \ln\left(\bar{Q}_n\right) + \boxed{5N\ln\left(\frac{\mathrm{SNR}_{\mathrm{net}}}{\sqrt{N}}\right)}\right] - \frac{5}{2}\mathscr{I}N\ln(\mathscr{I}) + \left(2 + \ln\frac{\sqrt{\det C_\Omega}}{V_\Omega}\right)$$

- Main scaling: $\ln \mathscr{B}_{\mathcal{S},\mathcal{G}} \sim \mathscr{I} N \ln \mathrm{SNR}_{\mathrm{net}}$
  - (i) $\mathscr{I}$: number of detectors
  - (ii) N : number of wavelets (i.e. model complexity)
  - (iii) $\mathrm{SNR}_{\mathrm{net}}$: signal-to-noise ratio

Lee et al., Phys. Rev. D **103**, 062002 (2021)

EMPIRICAL SCALING:
SINE-GAUSSIAN INJECTIONS ($N = 1$)

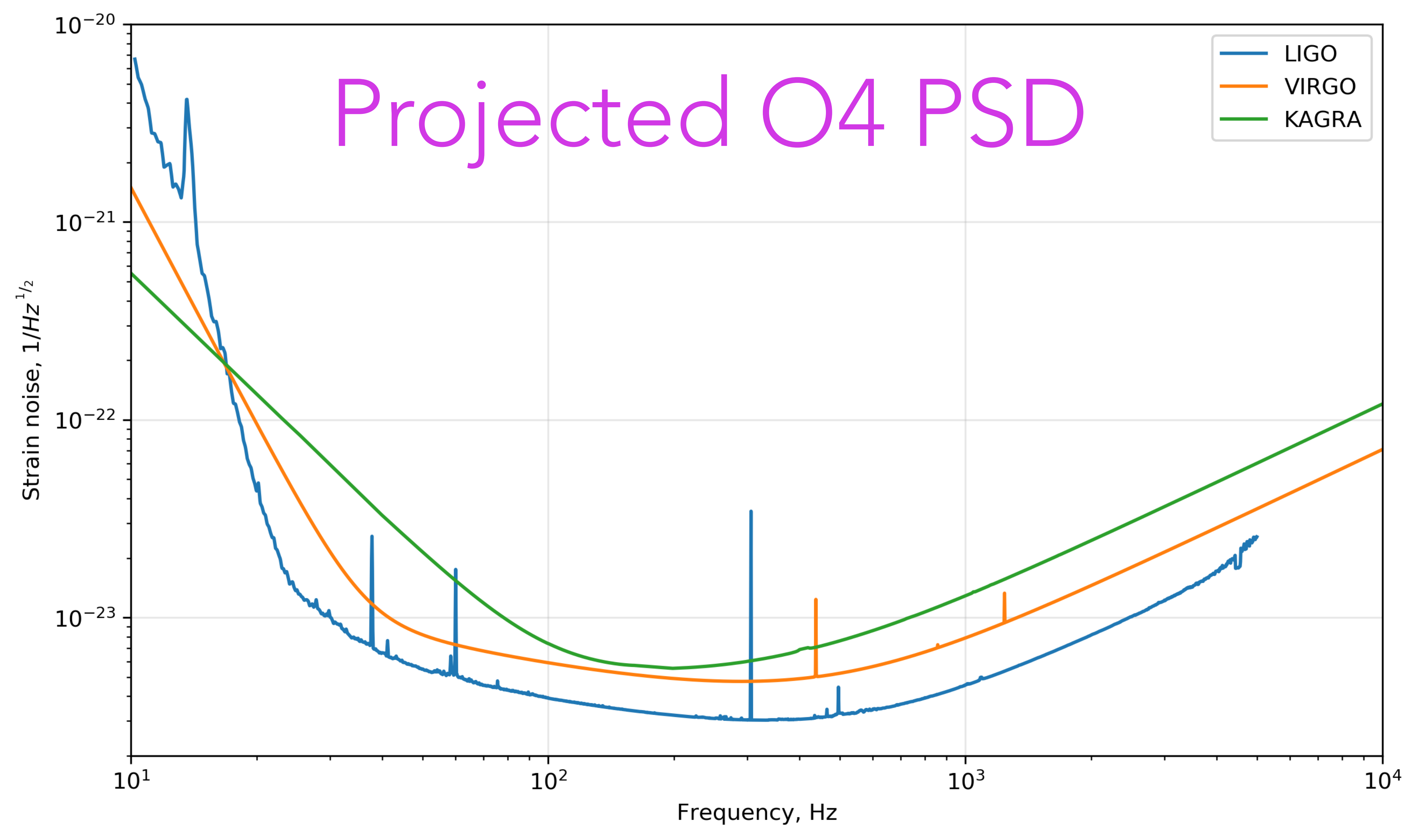

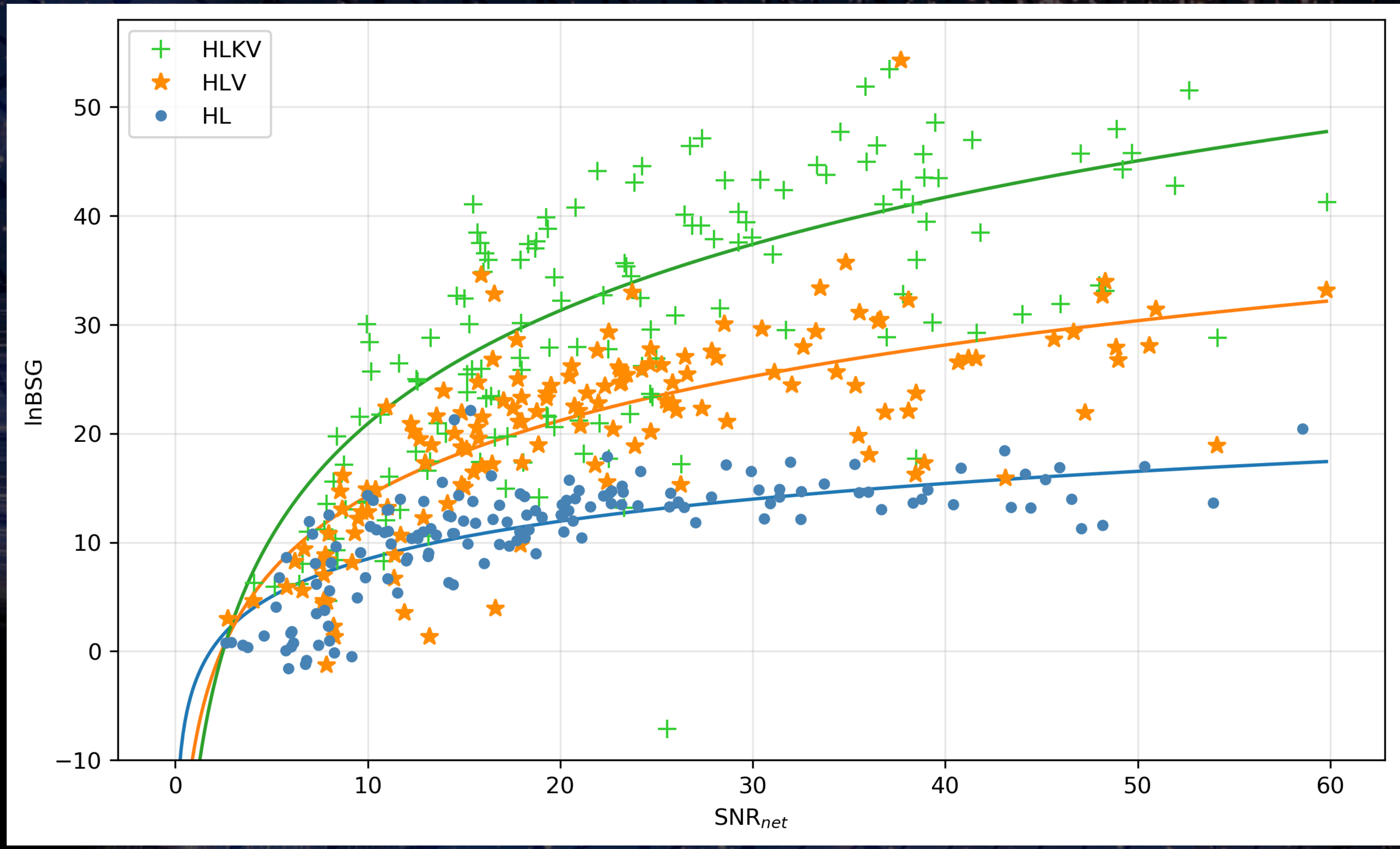

$$\ln \mathcal{B}_{\mathcal{S},\mathcal{G}} \simeq (\mathcal{I}-1)\left[\frac{5N}{2} + N\ln(V_\lambda) - \sum_n^N \ln\left(\bar{Q}_n\right) + 5N\ln\left(\frac{\mathrm{SNR_{net}}}{\sqrt{N}}\right)\right] - \frac{5}{2}\mathcal{I}N\ln(\mathcal{I}) + \left(2 + \ln\frac{\sqrt{\det C_\Omega}}{V_\Omega}\right)$$

for $N = 1$ simplifies to:

$$\ln \mathcal{B}_{\mathcal{S},\mathcal{G}} \approx (\mathcal{I}-1)[5\ln \mathrm{SNR_{net}} + c] + \frac{5}{2}\mathcal{I}\ln\mathcal{I} + d$$

EMPIRICAL SCALING: BINARY BLACK HOLE INJECTIONS

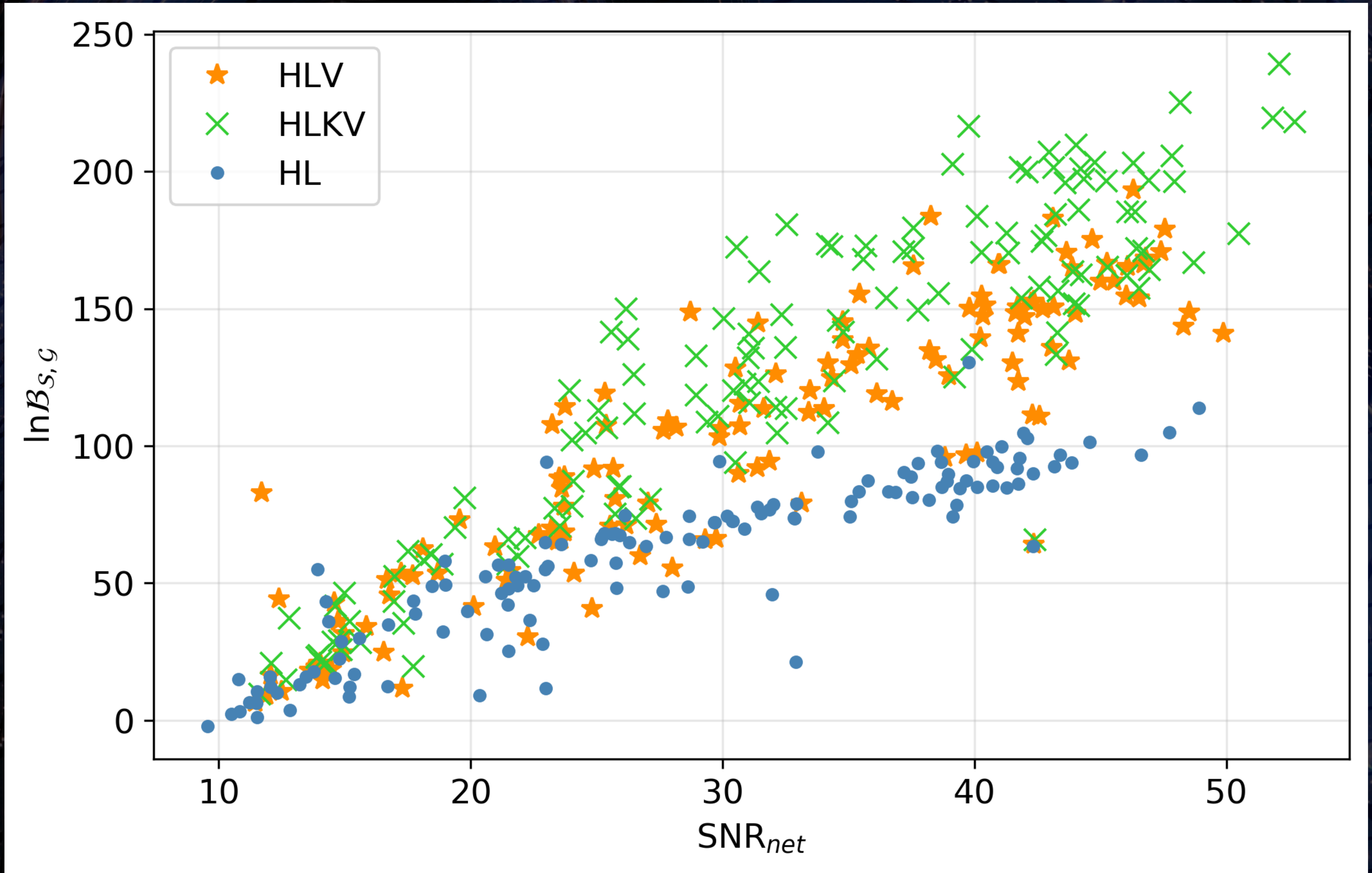

At comparable $\mathrm{SNR}_{\mathrm{net}}\ldots$

$\ln \mathscr{B}_{\mathscr{S},\mathscr{G}}$ increases as the number of detector $\mathscr{I}$ increases

✅ Consistent with $\ln \mathscr{B}_{\mathscr{S},\mathscr{G}} \sim \mathscr{I} N \ln \mathrm{SNR}_{\mathrm{net}}$

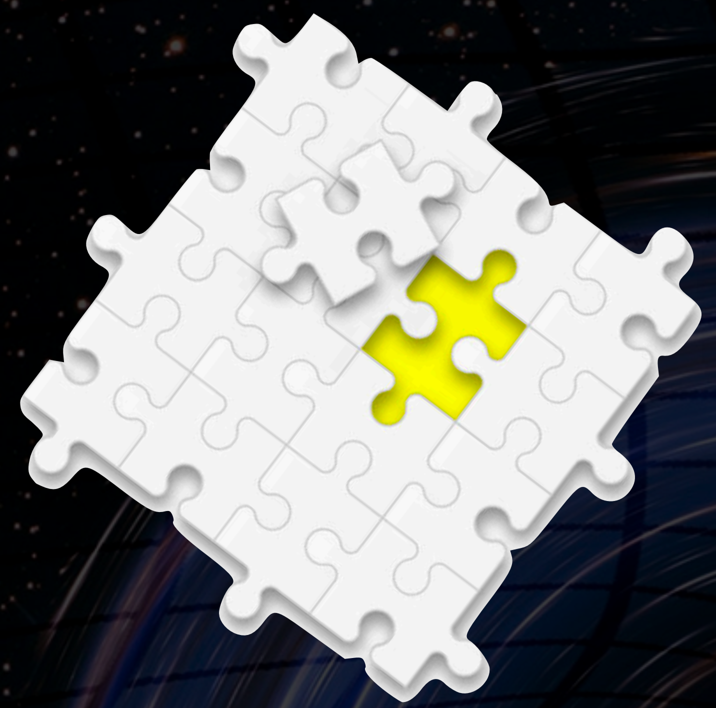

THE MISSING PUZZLE PIECE

- This work studies the improvement in $\ln \mathscr{B}_{\mathcal{S},\mathcal{G}}$ of astrophysical triggers with expanded detector networks
- BUT…
  Larger detector networks are more susceptible to instrumental glitches i.e. noisier detector backgrounds!

PART IB:

IMPACT OF NOISE TRANSIENTS ON GW BURST DETECTION EFFICIENCY OF *BAYESWAVE*

arXiv:2403.16837 (2024)

AIM OF THIS WORK

- Study the overall performance of *BayesWave* by accounting for the noise background
- Compare performance between:
  - Hanford-Livingston (HL), 2-detector network
  - Hanford-Livingston-Virgo (HLV), 3-detector network

FALSE ALARM PROBABILITY, P_{FA}

/measure of detection significance/

Probability that a trigger event with a given detection statistic ($\ln \mathscr{B}_{\mathscr{S},\mathscr{G}}$) is a false alarm **i.e. non-astrophysical**

Lower P_{FA} = Higher astrophysical significance

DETECTION EFFICIENCY P_{det}

/figure of merit for *BayesWave's* overall performance/

Probability of detecting an **astrophysical** event with a given significance (P_{FA})

EFFICIENCY CURVES

To characterise

DETECTION EFFICIENCY P_{det}

as a function of

FALSE ALARM PROBABILITY P_{FA}

Method adapted from Kanner et al, Phys. Rev. D 93, 022002 (2016)

EFFICIENCY CURVE "RECIPE"

2 COMPONENTS:

(1) **NOISE BACKGROUND MEASUREMENTS** → P_{FA}

- Distribution of *BayesWave*'s detection statistics $\ln \mathcal{B}_{\mathcal{S},\mathcal{G}}$ for **non-astrophysical triggers**

(2) **ASTROPHYSICAL MEASUREMENTS** → P_{det}

- As above, but for **astrophysical triggers**
- Compare with noise background measurements to get P_{det}

EFFICIENCY CURVE:
(1) NOISE BACKGROUND MEASUREMENT

EFFICIENCY CURVE:
(1) NOISE BACKGROUND MEASUREMENT

STEP 1: Down-selecting background triggers

- From Coherent WaveBurst (cWB) trigger lists of O3a time-slide data

HOW?

Fraction of randomly selected triggers satisfying $\rho \geq 7$

ρ scales with signal-to-noise ratio (SNR)

- HL → 1008 triggers
- HLV → 1134 triggers

EFFICIENCY CURVE: (1) NOISE BACKGROUND MEASUREMENT

STEP 2: Identifying Gaussian-noise-like background triggers

- Events more consistent with the Gaussian-noise model, $\mathscr{N}$ than the Gaussian-noise plus signal model, $\mathscr{S}$:

$$\ln \mathscr{B}_{\mathscr{S},\mathscr{N}} - \Delta \ln \mathscr{B}_{\mathscr{S},\mathscr{N}} \leq 0$$

- Meaningless to compare odds between signal and glitch models via $\ln \mathscr{B}_{\mathscr{S},\mathscr{G}}$
- Cannot remove from dataset as they still satisfy $\rho \geq 7$
- Assign arbitrarily low detection statistics: $\ln \mathscr{B}_{\mathscr{S},\mathscr{G}} = -500$

EFFICIENCY CURVE:
(1) NOISE BACKGROUND MEASUREMENT

STEP 3: Calculate P_{FA} as a function of $\ln \mathscr{B}_{\mathcal{S},\mathcal{G}}$

P_{FA}
/probability of false alarm/

Per-trigger probability (i.e. fraction) of non-astrophysical triggers detected above a given $\ln \mathscr{B}_{\mathcal{S},\mathcal{G}}$ threshold

Why not False alarm RATE (FAR)?

- FAR is a time-averaged quantity
- The timescales of HL and HLV time-slide background data are different

- P_{FA} is time-independent and marginalises over the number of triggers analysed is more suitable for comparison between the two networks

EFFICIENCY CURVE:
(1) NOISE BACKGROUND MEASUREMENT

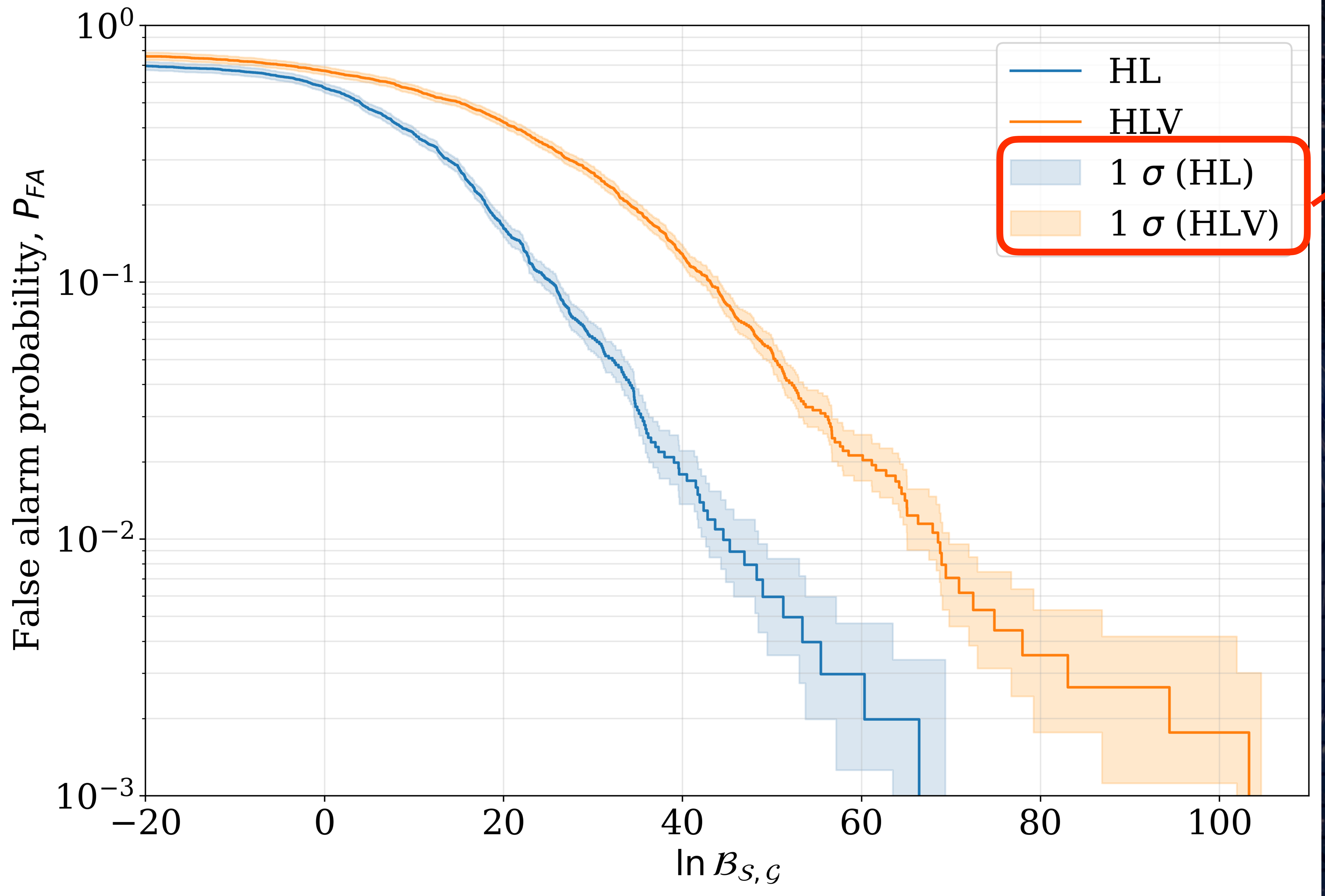

STEP 4: Error bars

Assume Poisson process

s.t.

1-σ in background event counts, $n = \sqrt{n}$

$\therefore$

1-σ in P_{FA} is $\dfrac{\sqrt{n}}{N}$

N: Total number of triggers (1008 in HL, 1134 in HLV)

X

EFFICIENCY CURVE:
(1) NOISE BACKGROUND MEASUREMENT

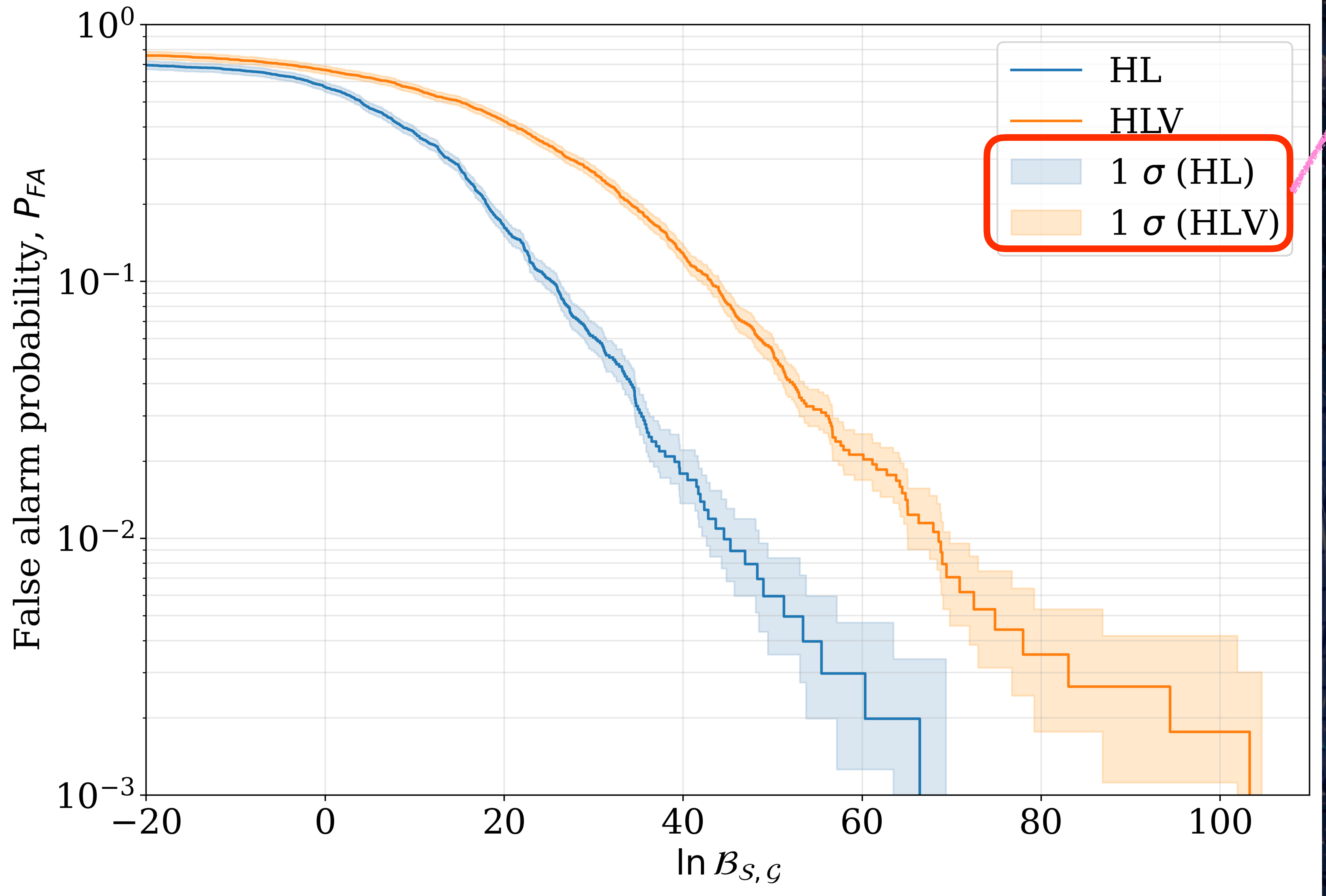

Poisson uncertainty region

Assuming background noise is a Poisson process

P_{FA} in HLV is higher than HL for all $\ln \mathcal{B}_{\mathcal{S},\mathcal{G}}$

i.e. HLV background is NOISIER than HL

Consistent with cWB

Szczepańczyk et al. (2022)

EFFICIENCY CURVE:

(2) ASTROPHYSICAL MEASUREMENTS WITH PHENOMENOLOGICAL INJECTIONS

EFFICIENCY CURVE:
(2) ASTROPHYSICAL MEASUREMENTS

Properties of injected events

- **Phenomenological binary black hole (BBH) waveforms**
- 1200 injections
- Equal component masses $30M_{\odot}$
- Randomly sampled distances such that the network SNR is within range $10 \leq \mathrm{SNR}_{\mathrm{net}} \leq 50$
- Uniform sky location, inclination and polarisation
- **Injected into** randomly selected segments throughout all of **O3a**

EFFICIENCY CURVE: (2) ASTROPHYSICAL MEASUREMENTS

Filtering non-detections

- O3a data is noisier than simulated HLV data,
  ∴ Injected $\mathrm{SNR}_{\mathrm{net}}$ are lower than the range $10 \leq \mathrm{SNR}_{\mathrm{net}} \leq 50$
- Nominal *BayesWave* significance threshold
  Only follow-up events with $\mathrm{SNR}_{\mathrm{net}} \geq 10$
  c.f. Only followed-up cWB (background) events with $\rho \geq 7$
- 790 events left → **The denominator of P_{det}**

EFFICIENCY CURVE:
(2) ASTROPHYSICAL MEASUREMENTS

IS1 Gaussian-noise-like events

- Events that satisfy $\mathrm{SNR}_{\mathrm{net}} \geq 10$
- But are more consistent with Gaussian noise

  i.e. $\ln \mathscr{B}_{\mathcal{S},\mathcal{N}} - \Delta \ln \mathscr{B}_{\mathcal{S},\mathcal{N}} \leq 0$
- Retained in IS1 but…

  Assign arbitrarily low detection statistics: $\ln \mathscr{B}_{\mathcal{S},\mathcal{G}} = -500$

  (same as background triggers)

X

EFFICIENCY CURVE:
(2) ASTROPHYSICAL MEASUREMENTS

Distribution of BBH injections

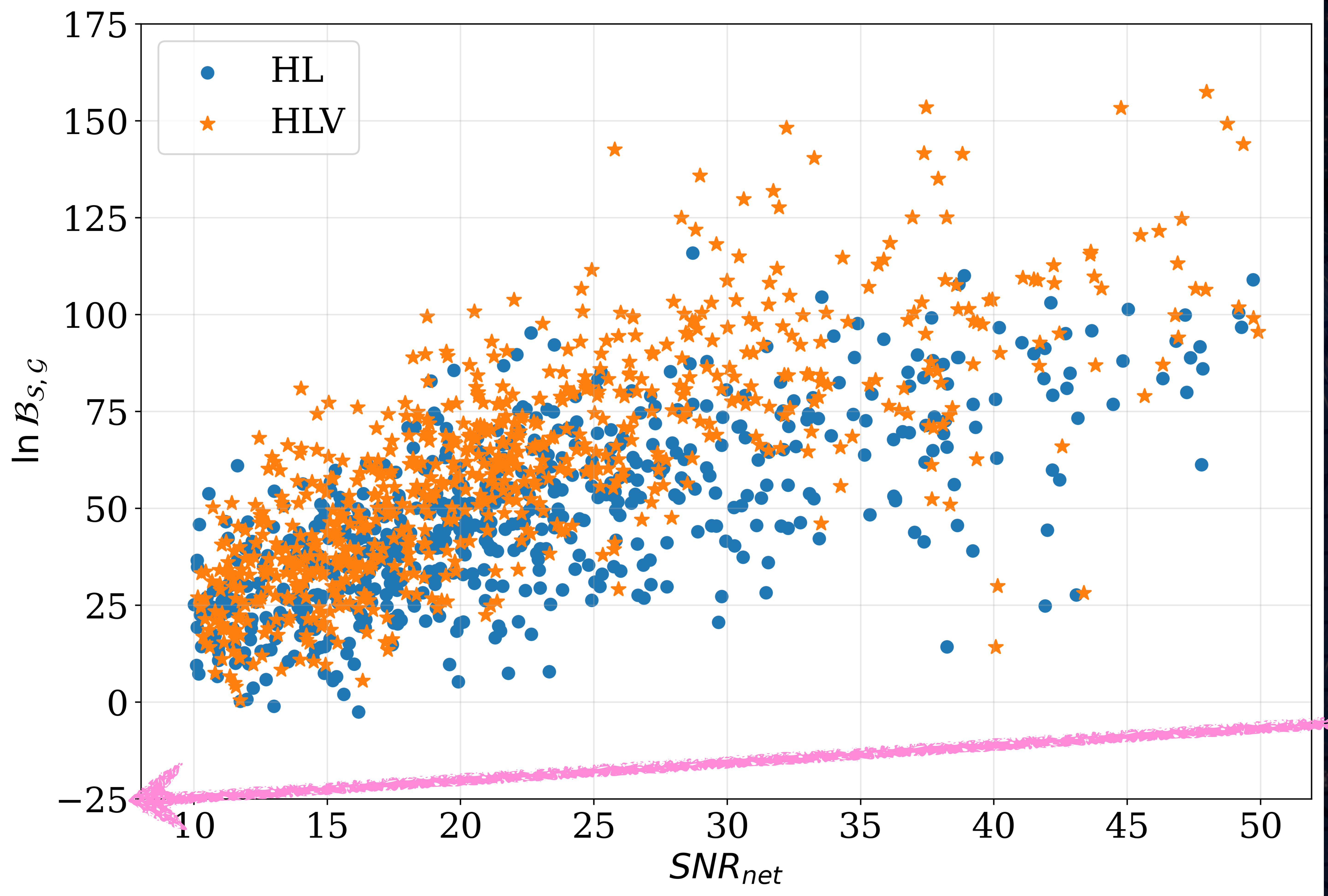

Consistent with previous work:

$$\ln \mathscr{B}_{\mathcal{S},\mathcal{G}} \sim \mathcal{I} N \ln \mathrm{SNR}_{\mathrm{net}}$$

$\ln \mathscr{B}_{\mathcal{S},\mathcal{G}} = -500$ events not shown

CONSTRUCTING EFFICIENCY CURVE

$P_{\rm FA} = 0.2$

/probability of false alarm/

Fraction of non-astrophysical triggers detected above a given $\ln \mathscr{B}_{\mathcal{S},\mathcal{G}}$ threshold

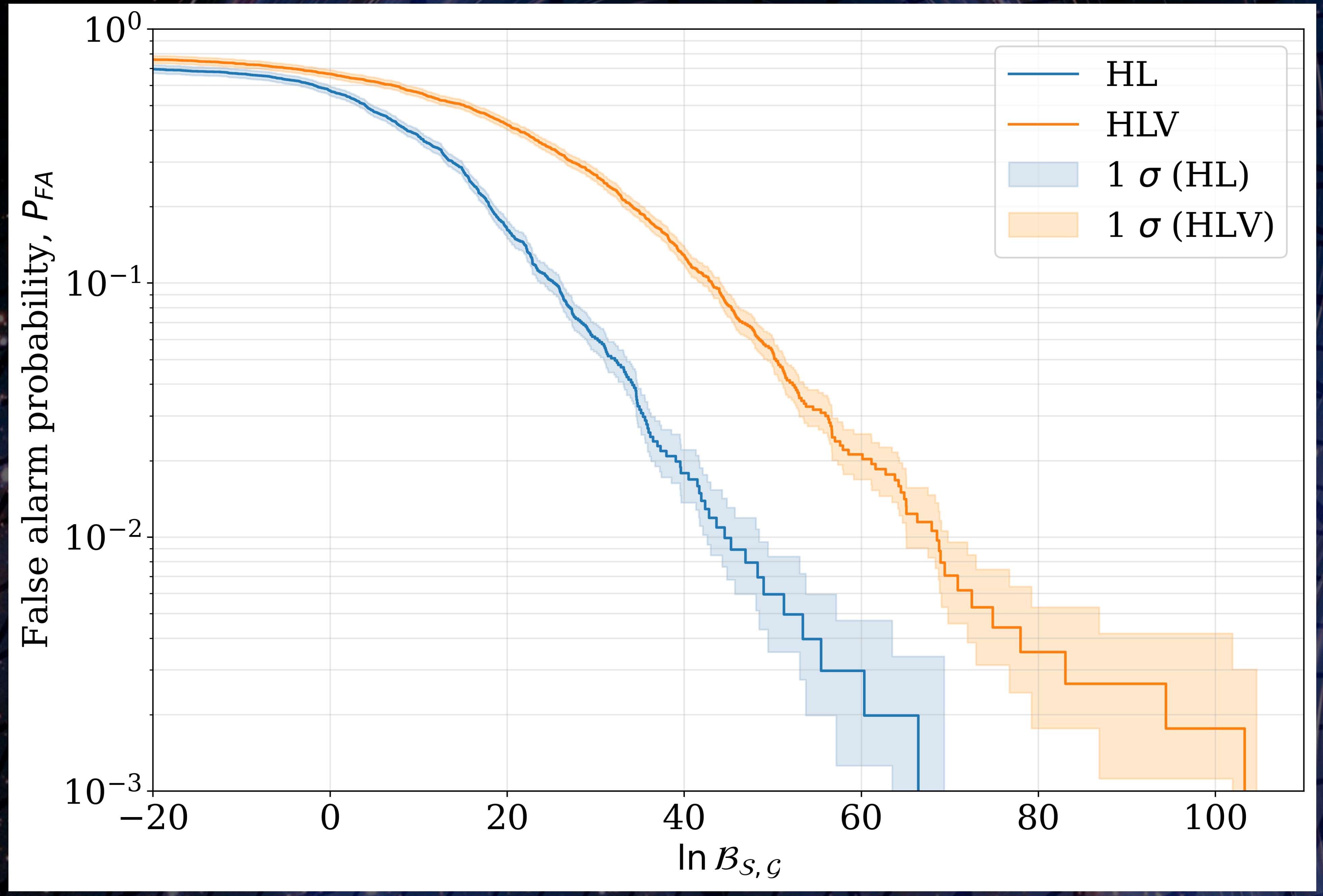

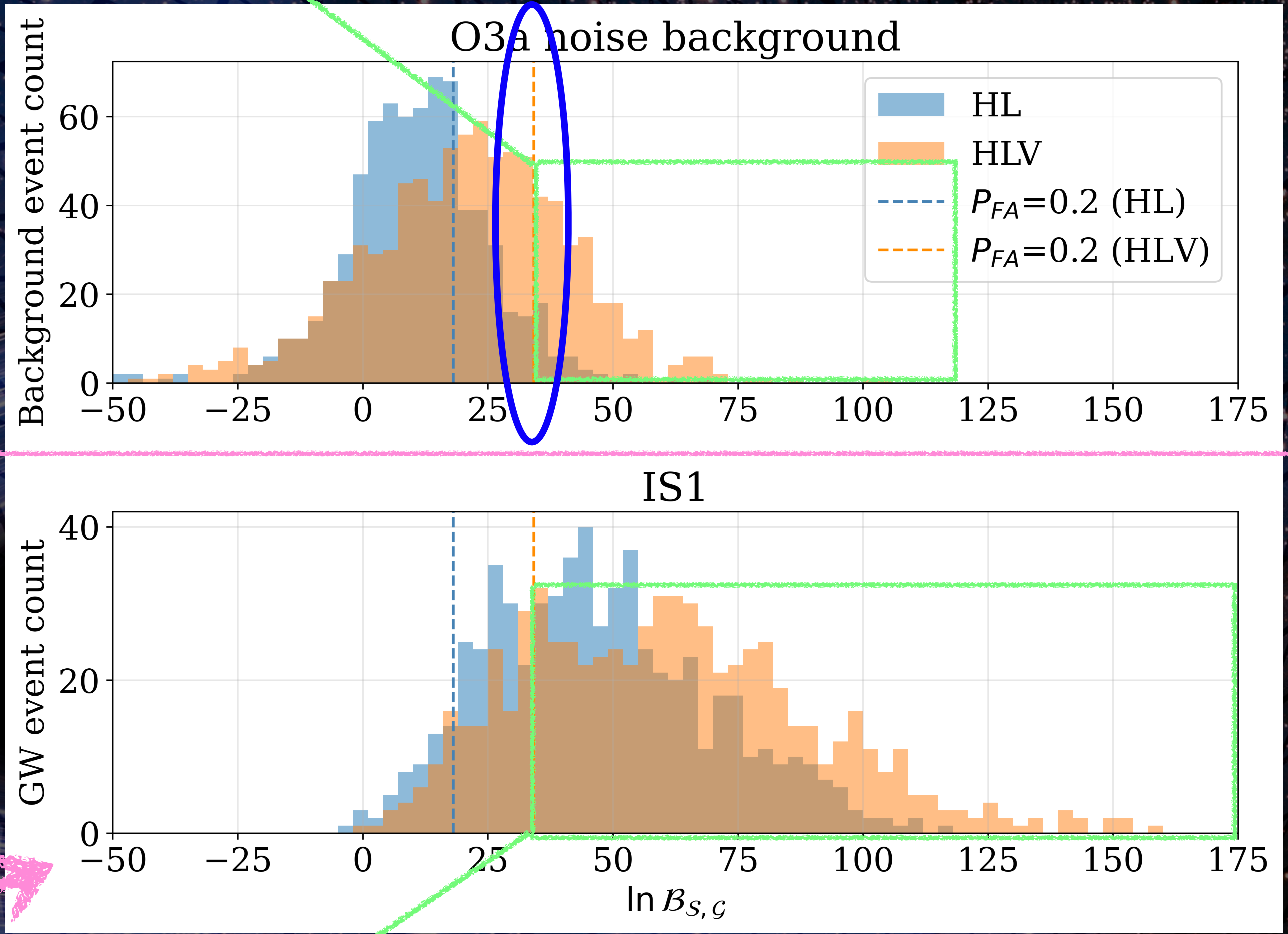

Again, $\ln \mathscr{B}_{\mathcal{S},\mathcal{G}} = -500$ events not shown

$P_{\rm det}$

/Detection efficiency/

Fraction of astrophysical events detected with significance i.e. $P_{\rm FA} \geq 0.2$

EFFICIENCY CURVES OF HL AND HLV

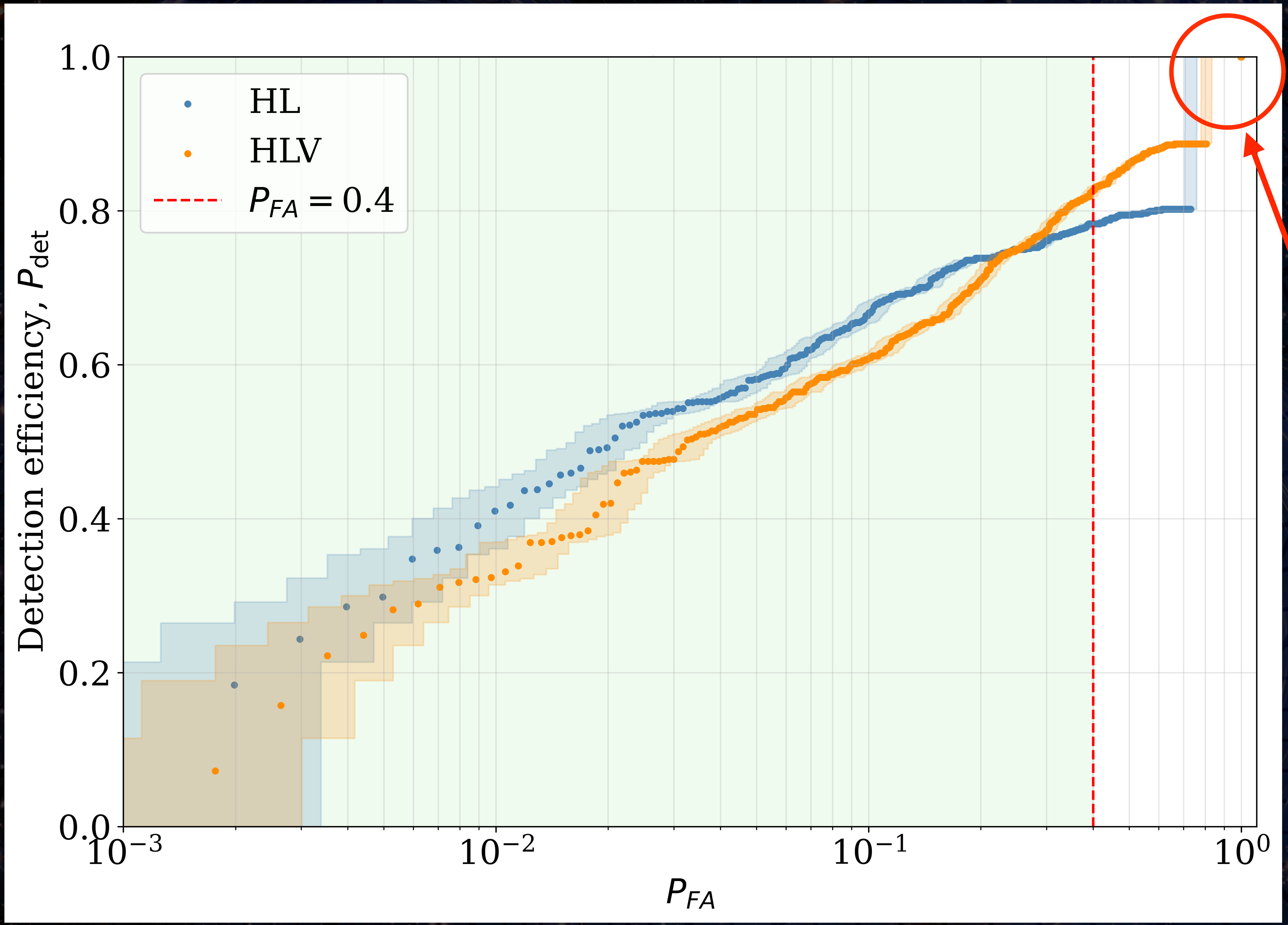

1-σ P_{FA} **POISSON UNCERTAINTY REGION**

same as background measurement

Cluster of Gaussian-noise-like events with

$\ln \mathscr{B}_{\mathscr{S},\mathscr{G}} = -500$ and $P_{\mathrm{FA}} = 1$

(i.e. minimal detection significance)

Practically meaningful regime $P_{\mathrm{FA}} \leq 0.4$

P_{det} of HL very slightly higher than HLV,

but the difference is not signifiant

P_{FA} AND $\ln \mathscr{B}_{\mathscr{S},\mathscr{G}}$ COMPARISON

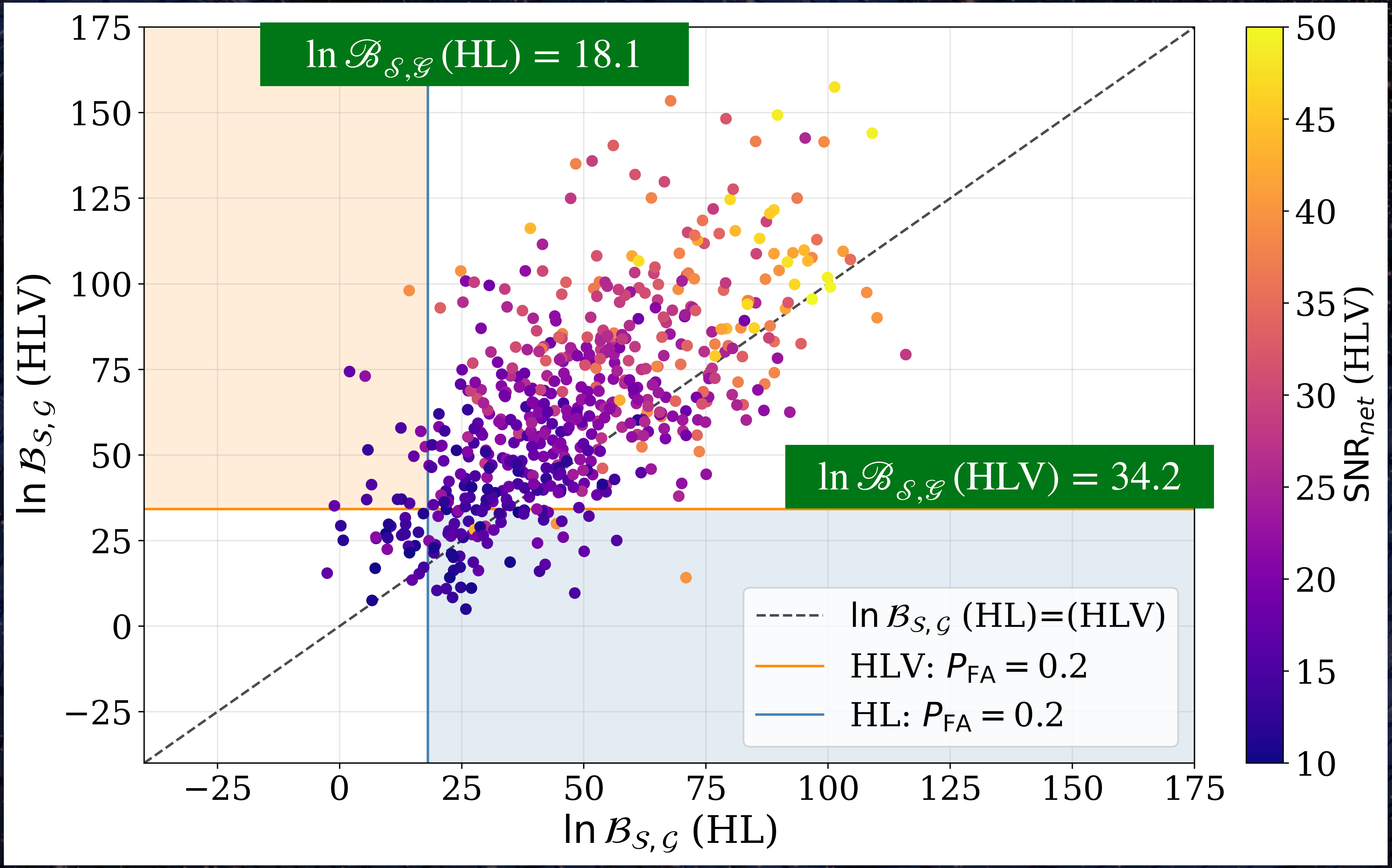

X

BAYESWAVE DETECTION SIGNIFICANCE OF **O3-LIKE COMPACT BINARY COALESCENCE (CBC) EVENTS**

O3-LIKE CBC INJECTIONS

To measure *BayesWave*'s detection significance of O3 GW candidates

Using the O3a HL and HLV backgrounds measured in this study

O3-LIKE CBC INJECTIONS

- Off-source waveforms
  - Waveform parameters sampled from match-filter posteriors of O3a/O3b candidate GW events
  - Injected in the proximity of the actual event
- 17 candidates from O3a, 5 candidates from O3b
  ** O3b waveforms are injected into random segments of O3a data
- 50 off-source waveforms per GW candidate
  i.e. (17+5) x 50 = 1100 injections

GWTC-2: Phys. Rev. X 11, 021053 (2021),
GWTC-3: arXiv:2111.03606 (2021).

O3-LIKE CBC INJECTIONS

Filtering injections

- **Non-detections:**
  - Only follow-up injections with $\mathrm{SNR}_{\mathrm{net}} \geq 10$

    c.f. Only followed-up cWB (background) events with $\rho \geq 7$
  - 4 (low match-filter SNR) GW candidates removed $\because \leq 25$ (less than half of) off-source waveforms satisfy *BayesWave*'s detection criteria
- **Gaussian-noise-like injections**
  - Assign arbitrarily low detection statistics: $\ln \mathscr{B}_{\mathcal{S},\mathcal{G}} = -500$

O3-LIKE CBC INJECTIONS

Visualising distributions of off-source injections

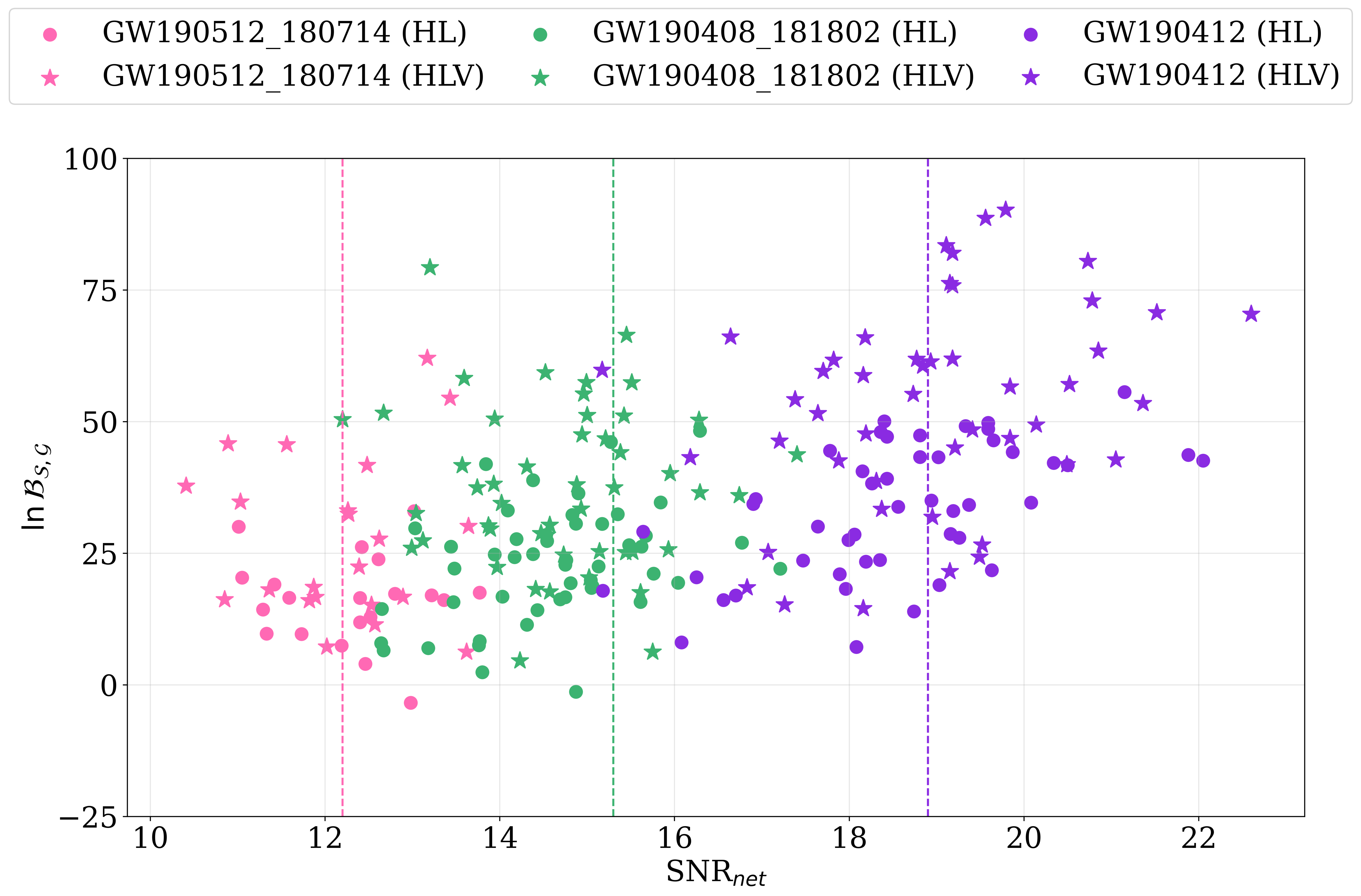

Median match-filter SNR

GW190512_180714 → 12.2

GW190408_181802 → 15.3

GW190412 → 18.9

BAYESWAVE DETECTION SIGNIFICANCE

REMAINING 18 O3-LIKE CBC INJECTIONS

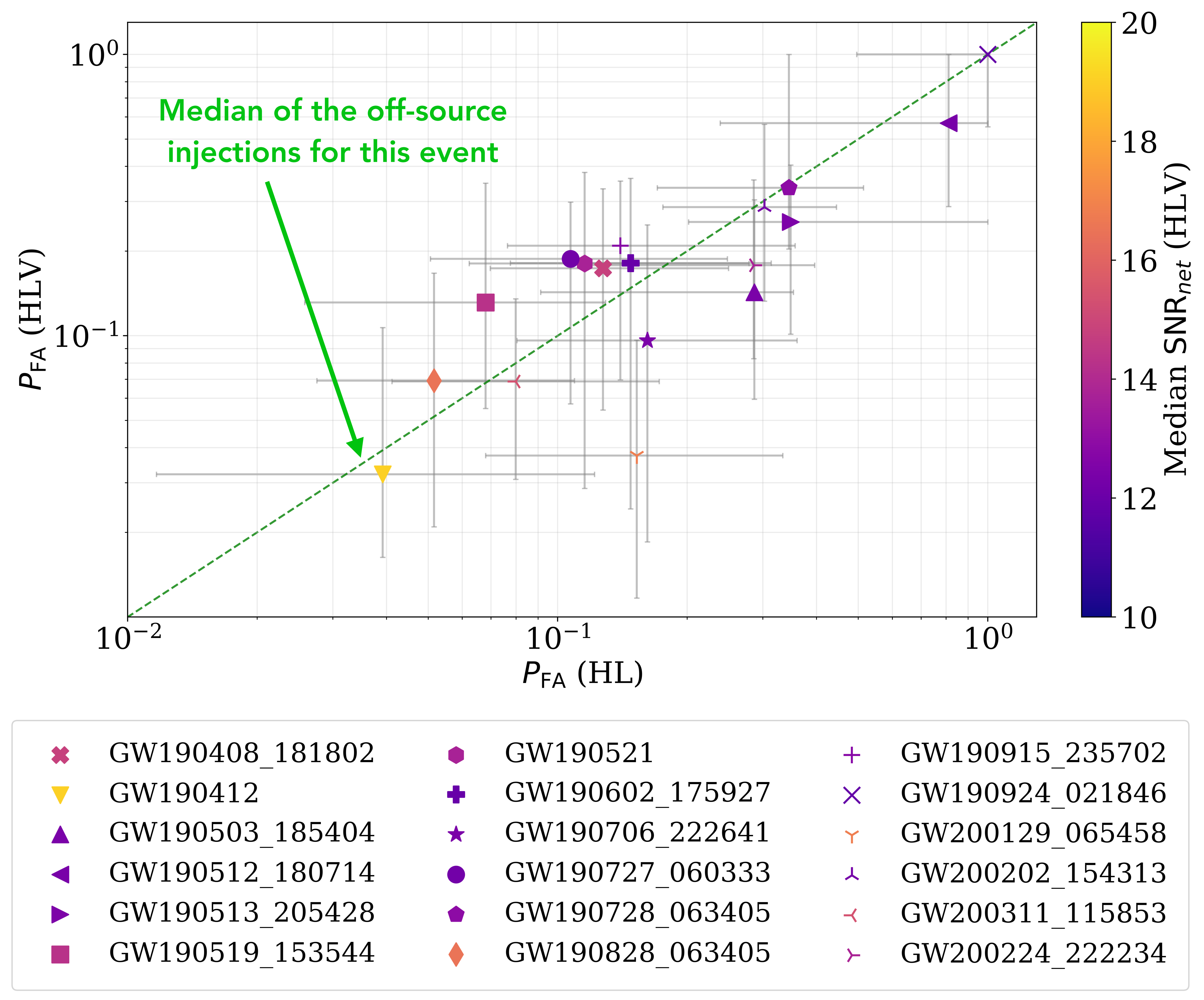

Error bars

IQR of P_{FA} within each GW candidate

All events are detected with comparable significance between HL and HLV

SUMMARY OF RESULTS

- **Both the phenomenological BBH injections and O3-like events show comparable *BayesWave* performance with HL and HLV at O3 sensitivities**
  - Although $\ln \mathscr{B}_{\mathscr{S},\mathscr{G}}$ increases with more detectors, false alarm probability P_{FA} is also higher (i.e. noisier detector backgrounds) $\therefore$ Larger detector networks need to attain higher $\ln \mathscr{B}_{\mathscr{S},\mathscr{G}}$ to achieve the same significance (P_{FA}) as smaller networks
- **Findings consistent with:**
  - LVK O3 all-sky burst search (Phys. Rev. D **104**, 122004)
  - cWB search, Szczepańzyk et al. 2022 (Phys. Rev. D **107**, 062002)

KEY TAKEAWAY

BayesWave's detection efficiency is comparable for two- and three-detector networks in O3

because

more frequent glitches in expanded detector networks offsets the advantage of higher detection statistics ($\ln \mathscr{B}_{\mathcal{S},\mathcal{G}}$)

Accepted PRD - arXiv:2403.16837 (2024)

PART II:

CHARACTERISATION OF GW BURST POLARISATIONS WITH *BAYESWAVE*

GW POLARISATIONS

- According to General Relativity, GWs have two polarisations
  - Plus (+)
  - Cross (×)

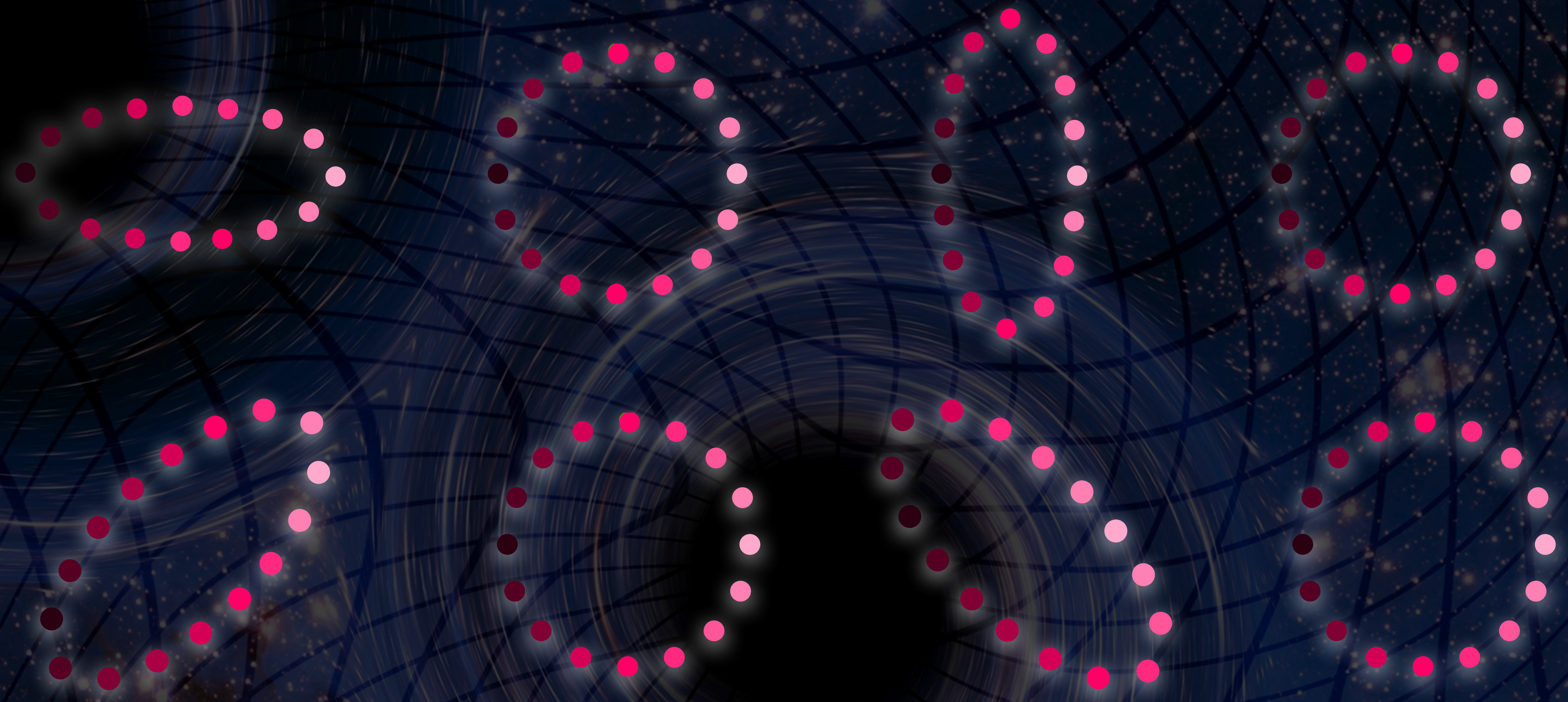

Deformation of a ring of free-falling particles by each polarisation modes

DISENTANGLING GW POLARISATIONS

- Antenna pattern functions : $F_\times(\Omega, \psi)$ and $F_+(\Omega, \psi)$
  - Sensitivity of a detector to each polarisation state
  - Ω = the sky location of the source
  - ψ = the polarization angle
- Interferometric response of detector I (in the frequency domain)
  - $\tilde{h}_I = \left[F_{\times,I}(\Omega, \psi)\tilde{h}_\times + F_{+,I}(\Omega, \psi)\tilde{h}_+\right] e^{2\pi i f \Delta t_I(\Omega)}$
  - $\tilde{h}_+$ and $\tilde{h}_\times$ = amplitudes at a nominal reference location
  - Δt_I = light travel time from the reference location to detector I

THE POLARISATION ANGLE ψ

- Arbitrarily defined w.r.t to a reference direction: west of celestial equator
- Z is the direction of propagation of the GW
- X is the x-axis of the wave plane
  - $\psi = 0$ if X is parallel to the reference direction
- X and Y are the directional vectors used to define the polarisation components

$$h_+ = \frac{1}{2}\left(\hat{x}_i\hat{x}_j - \hat{y}_i\hat{y}_j\right) h^{ij} \qquad h_\times = \frac{1}{2}\left(\hat{x}_i\hat{y}_j + \hat{y}_i\hat{x}_j\right) h^{ij}$$

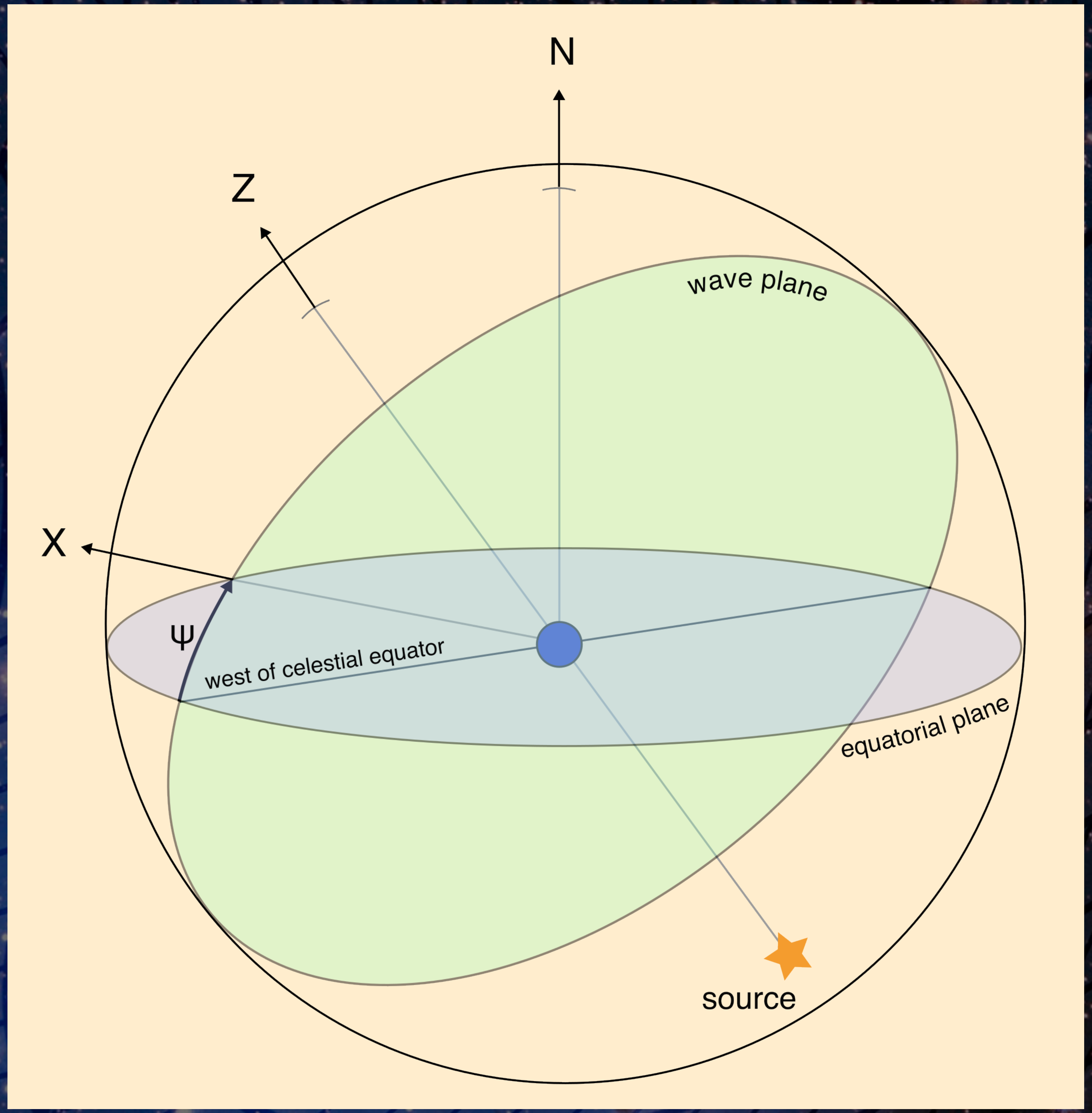

[Adapted from Header LALSimulation.h (coordinate systems)]

DISENTANGLING GW POLARISATIONS

$$\tilde{h}_I = \left[F_\times(\Omega, \psi)\tilde{h}_\times + F_+(\Omega, \psi)\tilde{h}_+ \right] e^{2\pi i f \Delta t(\Omega)}$$

- Contains up to four unknowns:
  - The two polarisation modes
  - Sky location
  - Source orientation ψ
- Need responses from multiple detectors to extract the polarisation components

BAYESWAVE SIGNAL MODEL UPDATE

- Elliptical polarisation, **E**

$$\tilde{h}_+ = \sum_{n=1}^{N} \Lambda\left(f;\, t_0^n, f_0^n, Q^n, A^n, \phi^n\right)$$

$$\tilde{h}_\times = i\epsilon \tilde{h}_+$$

- Relaxed polarisation, **R**

$$\tilde{h}_+ = \sum_{n=1}^{N} \Lambda\left(f;\, \boxed{t_0^n, f_0^n, Q^n,} A^{n,+}, \phi^{n,+}\right)$$

$$\tilde{h}_\times = \sum_{n=1}^{N} \Lambda\left(f;\, \boxed{t_0^n, f_0^n, Q^n,} A^{n,\times}, \phi^{n,\times}\right)$$

To avoid degeneracies with the glitch model

Λ : wavelet

ϵ : ellipticity

N : number of wavelets in signal model

Cornish + Littenberg, Class. Quant. Grav 32, 130512 (2015)
Cornish et al., Phys. Rev. D 103, 044006 (2021)

WHY THE **RELAXED POLARIZATION** (**R**) MODEL?

- **E** does not hold for CBCs with time-varying polarisations, e.g.
  - Distinctive higher-order modes
  - Spin-precessing → Amplitude modulation
- Other transient signals like supernovae are also generally unpolarised

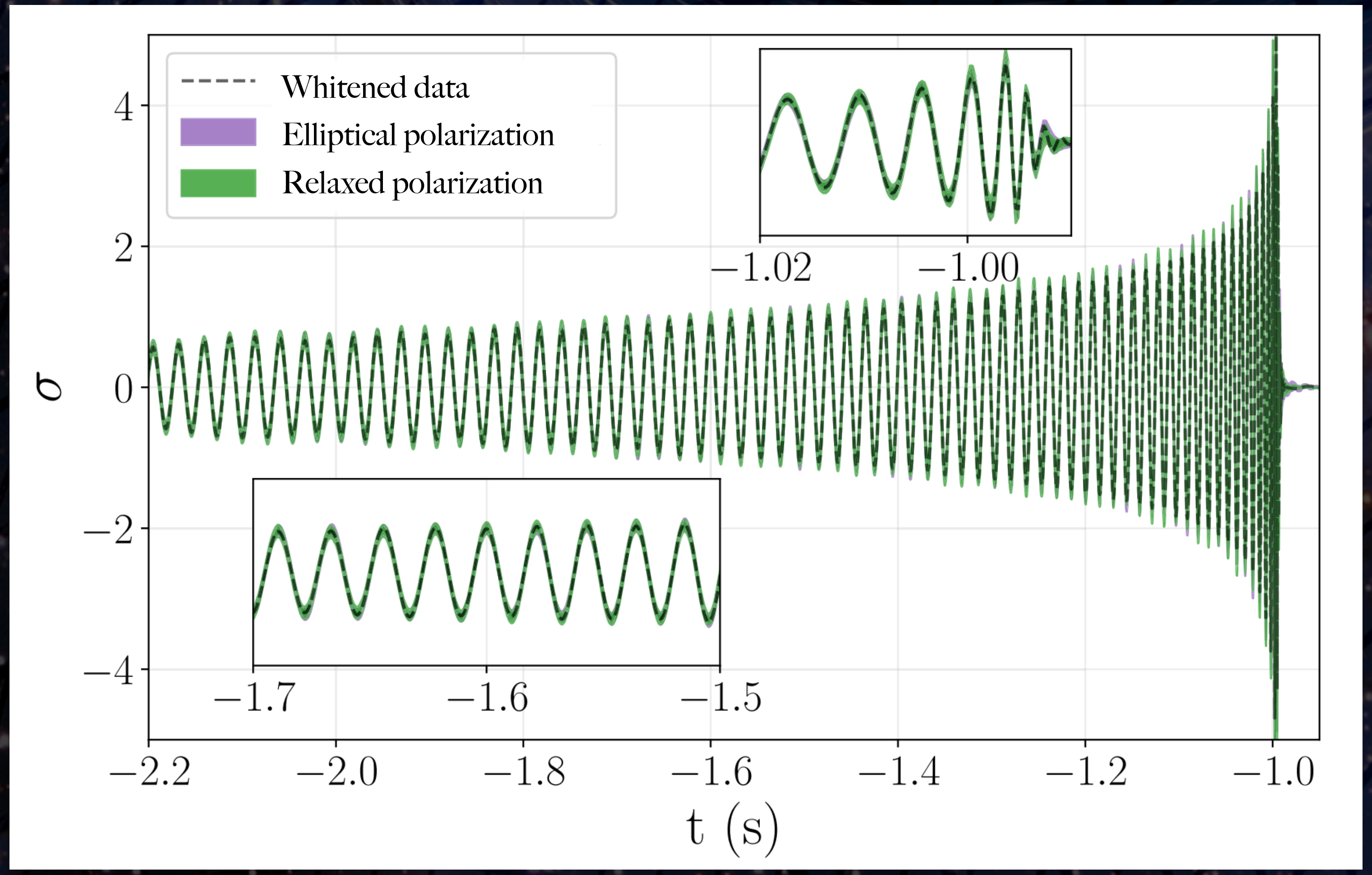

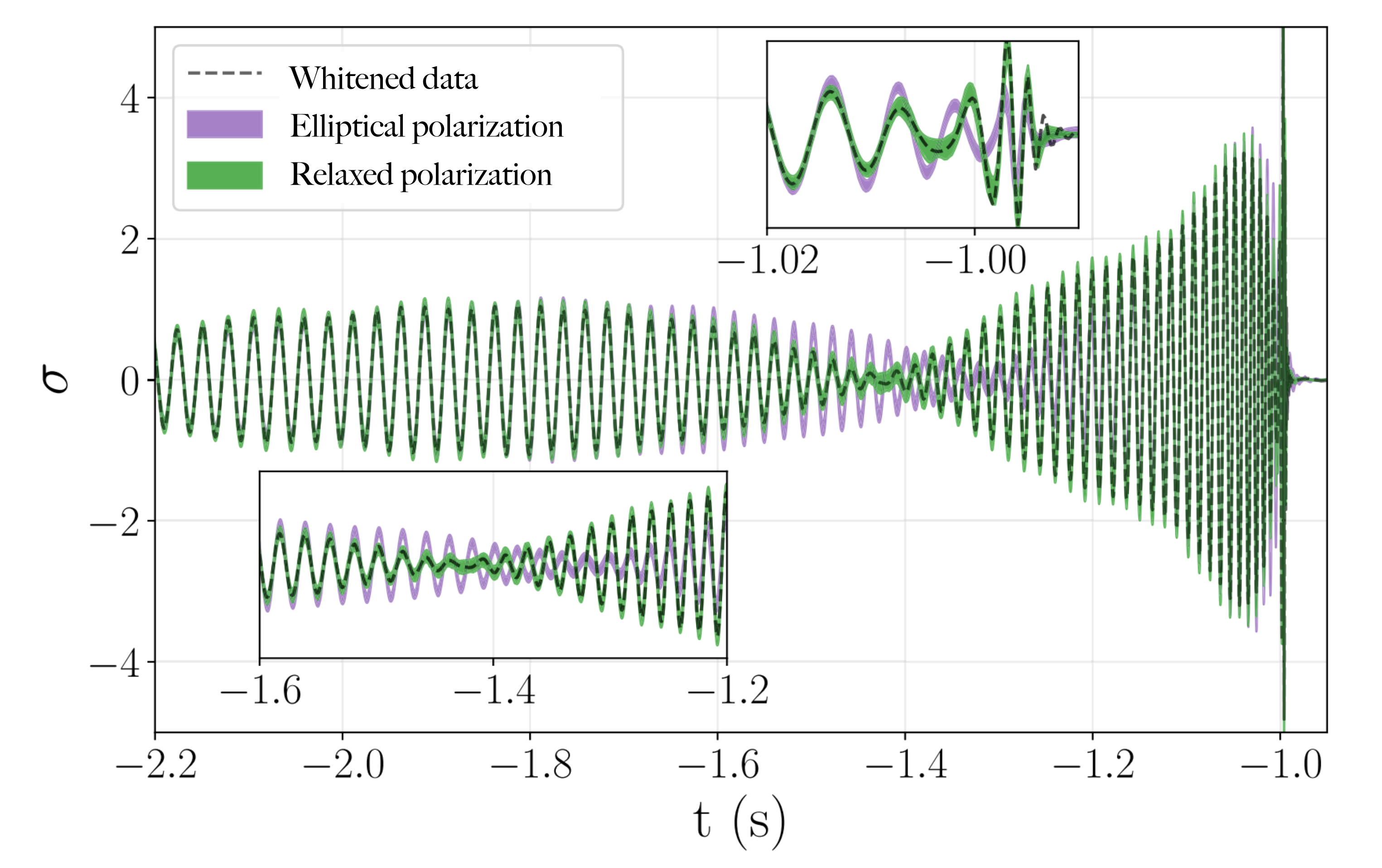

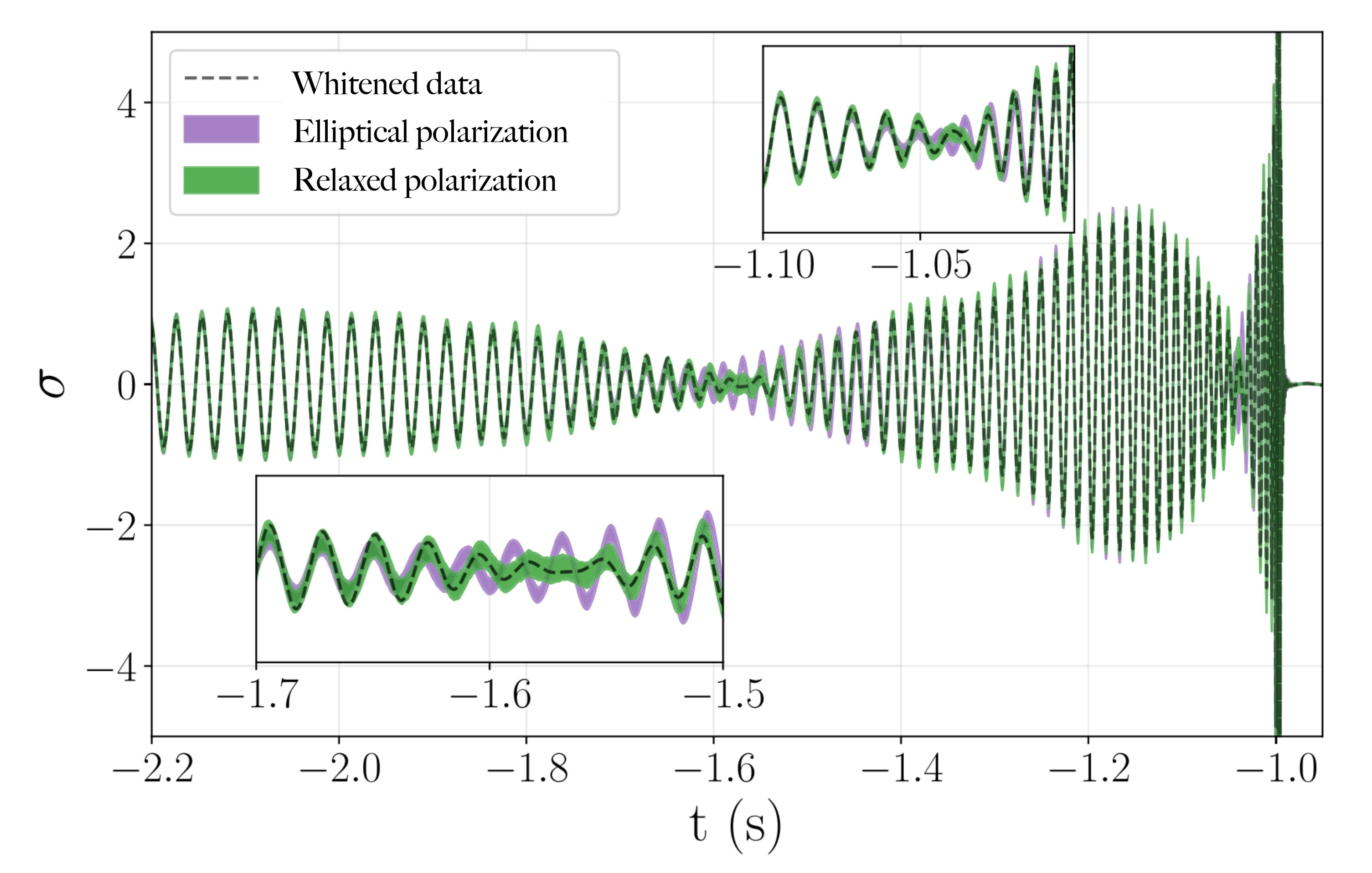

Cornish et al., Phys. Rev. D 103, 044006 (2021)

ELLIPTICAL (E) VS. RELAXED (R)

How well do the **E** and **R** polarization models represent GW signals from non-precessing and precessing binaries

TWO INJECTION SETS

- **IMRPhenomPv3 - Phenomenological (precessing) BBH waveforms**
- 200 injections
- High mass ratio $40M_{\odot} - 8M_{\odot}$
- Sampled distances such that the HLV $\mathrm{SNR}_{\mathrm{net}} \sim 50$ (loud and ideal!)
- Uniform sky location and polarisation angle
- **Injected into** simulated LIGO and Virgo noise

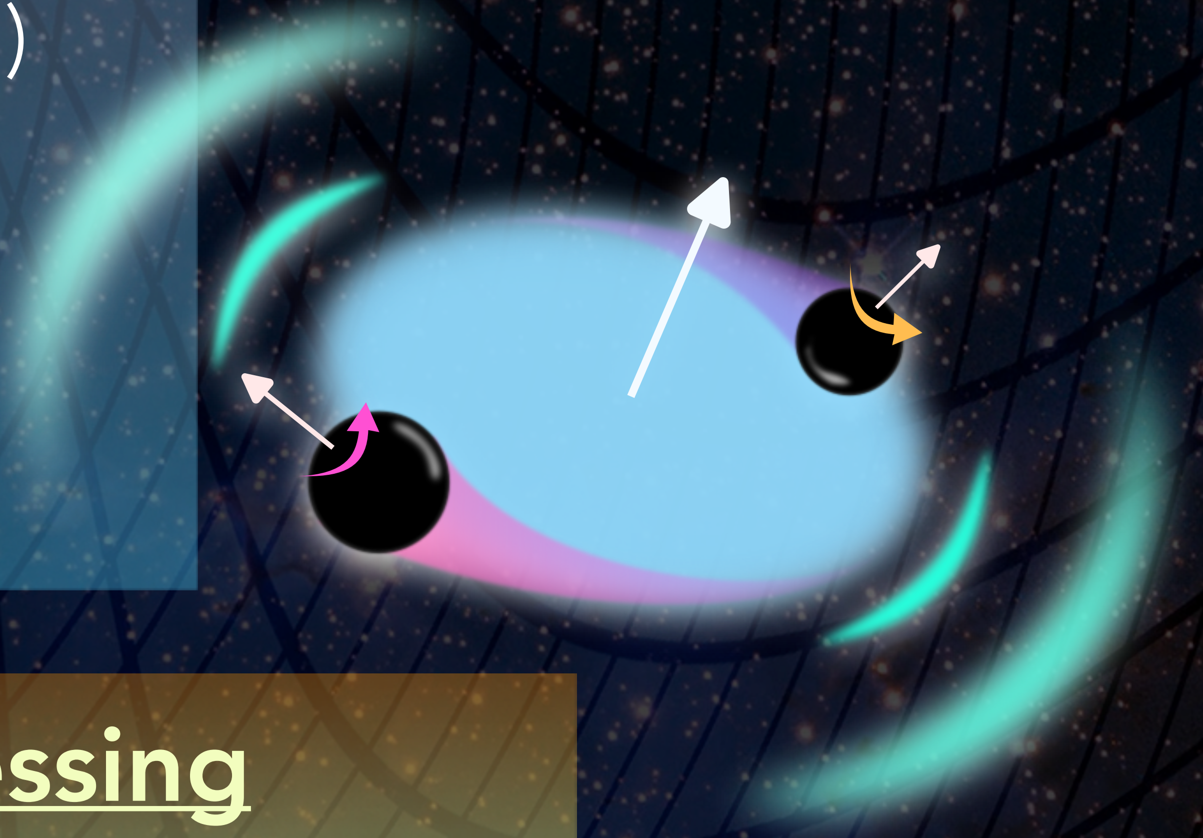

Non-precessing

- Fixed inclination at 45°
- Zero spin i.e. $|\vec{\chi}_i| = 0$;
  $\vec{\chi}_i = \vec{s}_i / m_i^2$ is the dimensionless spin parameter

Precessing

- Fixed *initial* inclination at 45°
- *Initial* spin for each component mass is independently sampled within $0.1 \leq |\vec{\chi}_i| \leq 1.0$

S. Khan et al. , Phys. Rev. D 100, 024059 (2019)

DIMENSIONLESS PRECESSION SPIN PARAMETER

$$\chi_p := \frac{\max(A_1 S_{1\perp}, A_2 S_{2\perp})}{A_1 m_1^2}$$

$$0 \leq \chi_p \leq 1$$

Non-zero when in-plane spin is present

i.e. spin components that are not (anti)parallel to the orbital angular momentum

COMPARING ELLIPTICAL (**E**) AND RELAXED (**R**)

Bayes Factor

$$\ln \mathscr{B}_{\mathbf{R},\mathbf{E}} = \ln p(\vec{s} \mid \mathbf{R}) - \ln p(\vec{s} \mid \mathbf{E})$$

Network overlap (i.e. match)

$$\mathcal{O}_{\mathbf{R},\mathbf{E}} = \frac{\sum_i \left(h^i_{\mathbf{R}} \mid h^i_{\mathbf{E}}\right)}{\sqrt{\sum_i \left(h^i_{\mathbf{R}} \mid h^i_{\mathbf{R}}\right) \sum_i \left(h^i_{\mathbf{E}} \mid h^i_{\mathbf{E}}\right)}}$$

where h^i is the *BayesWave*-recovered waveform for the i-th detector

(PRELIMINARY RESULTS)

HOW WELL DO THE E AND R POLARIZATION MODELS REPRESENT GW SIGNALS FROM NON-PRECESSING AND PRECESSING BINARIES

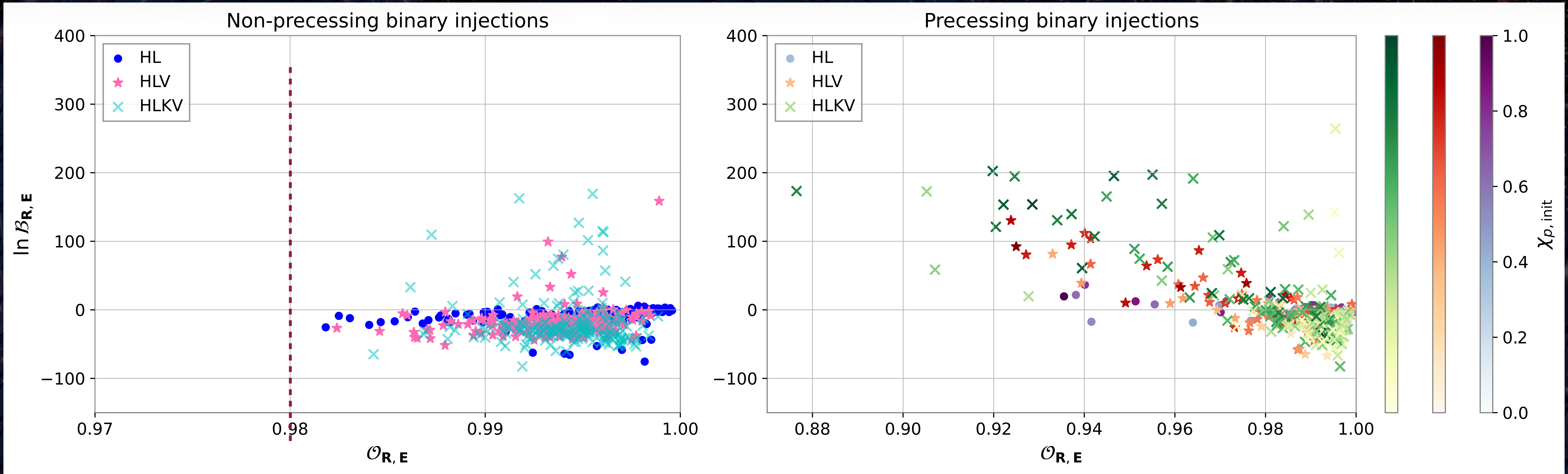

✅ Is it Gaussian noise?

$\ln \mathcal{B}_{\mathbf{R},\mathcal{N}}$ *and* $\ln \mathcal{B}_{\mathbf{E},\mathcal{N}} \geq 50$

✅ It is a glitch?

$\ln \mathcal{B}_{\mathbf{R},\mathcal{G}}$ *and* $\ln \mathcal{B}_{\mathbf{E},\mathcal{G}} \geq 20$

(PRELIMINARY RESULTS)

HOW WELL DO THE E AND R POLARIZATION MODELS REPRESENT GW SIGNALS FROM NON-PRECESSING AND PRECESSING BINARIES

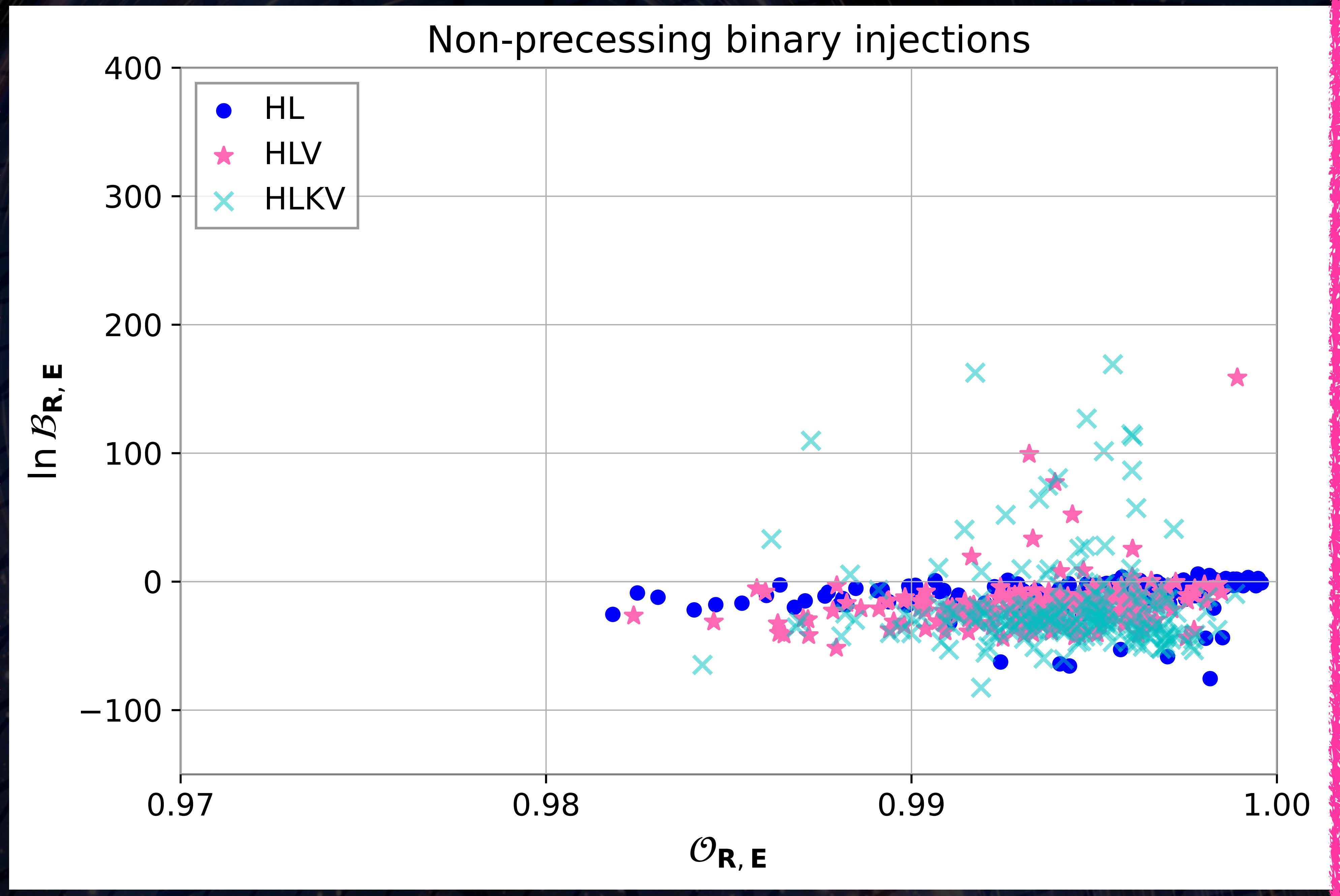

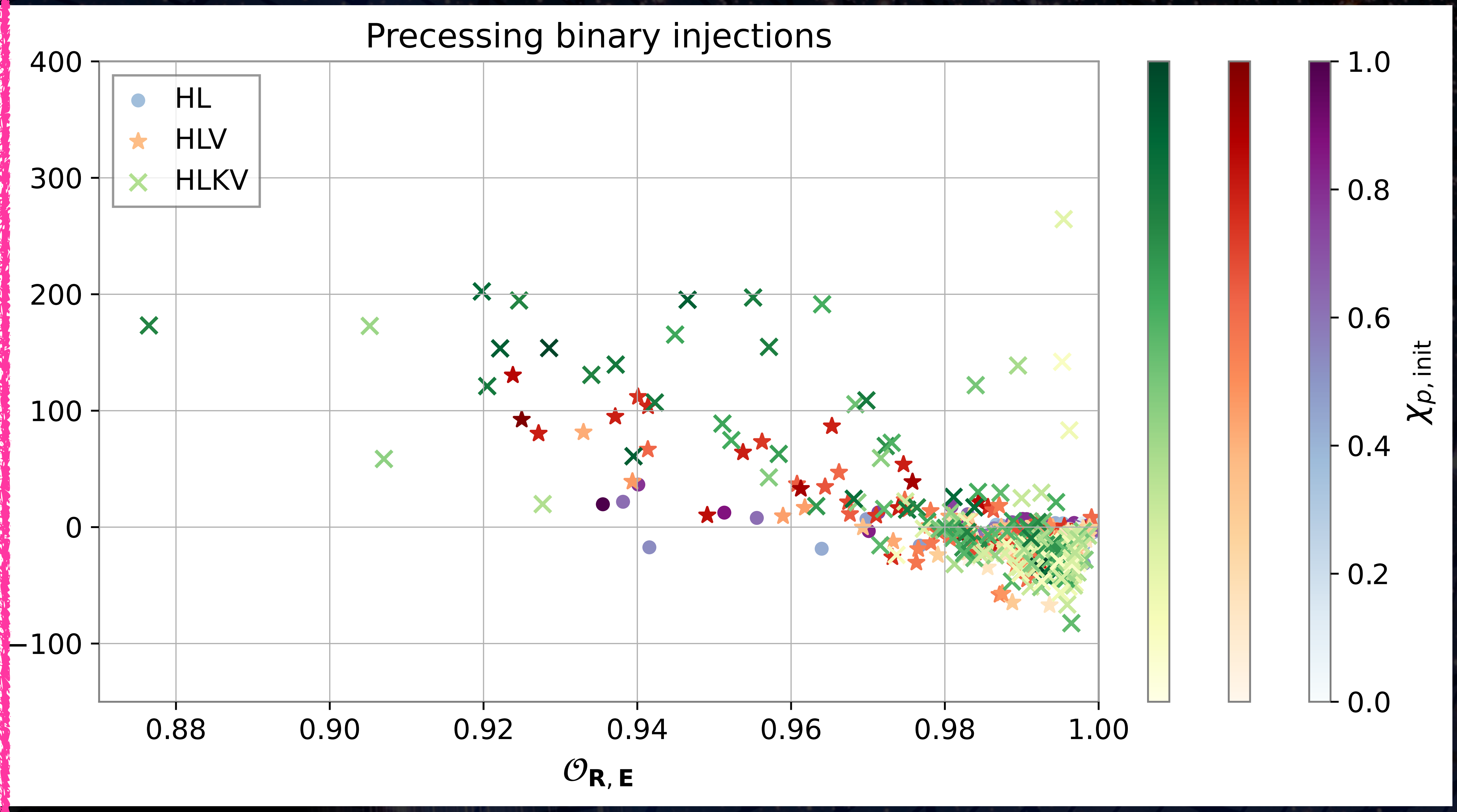

$$\text{Evidence of model } \mathscr{M} \simeq \text{Likelihood} \times \frac{\Delta V_{\mathscr{M}}}{V_{\mathscr{M}}}$$

$$\text{Bayes factor, } \mathscr{B}_{\mathbf{R,E}} \simeq \text{Likelihood ratio} \times \frac{\Delta V_{\mathbf{R}}}{\Delta V_{\mathbf{E}}} \frac{V_{\mathbf{E}}}{V_{\mathbf{R}}}$$

$\Delta V_{\mathscr{M}}$: Posterior volume

$V_{\mathscr{M}}$: Total parameter space volume of model $\mathscr{M}$

(PRELIMINARY RESULTS)

HOW WELL DO THE E AND R POLARIZATION MODELS REPRESENT GW SIGNALS FROM NON-PRECESSING AND PRECESSING BINARIES

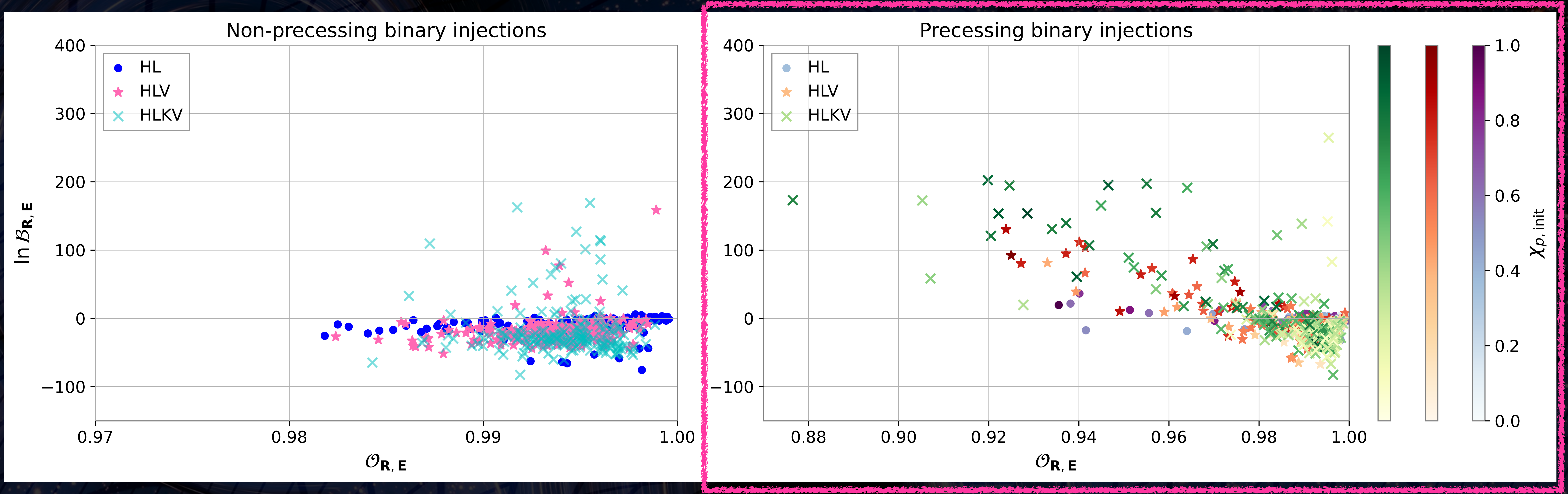

(1) Generally lower $\mathcal{O}_{\mathbf{R,E}}$ compared to the non-precessing binary injections, especially for events with higher $\chi_{p,\mathrm{init}}$

(2) $\ln \mathcal{B}_{\mathbf{R,E}}$ becomes increasingly positive as $\mathcal{O}_{\mathbf{R,E}}$ reduces $\Longrightarrow$ more evidence for **R**

(3) Increase in $\ln \mathcal{B}_{\mathbf{R,E}}$ is more prominent with larger detector networks

(PRELIMINARY RESULTS)

EVENTS WITH $\ln \mathscr{B}_{\mathbf{R,E}} \geq 0$ FOR NON-PRECESSING BINARIES WHAT DO THEY IMPLY?

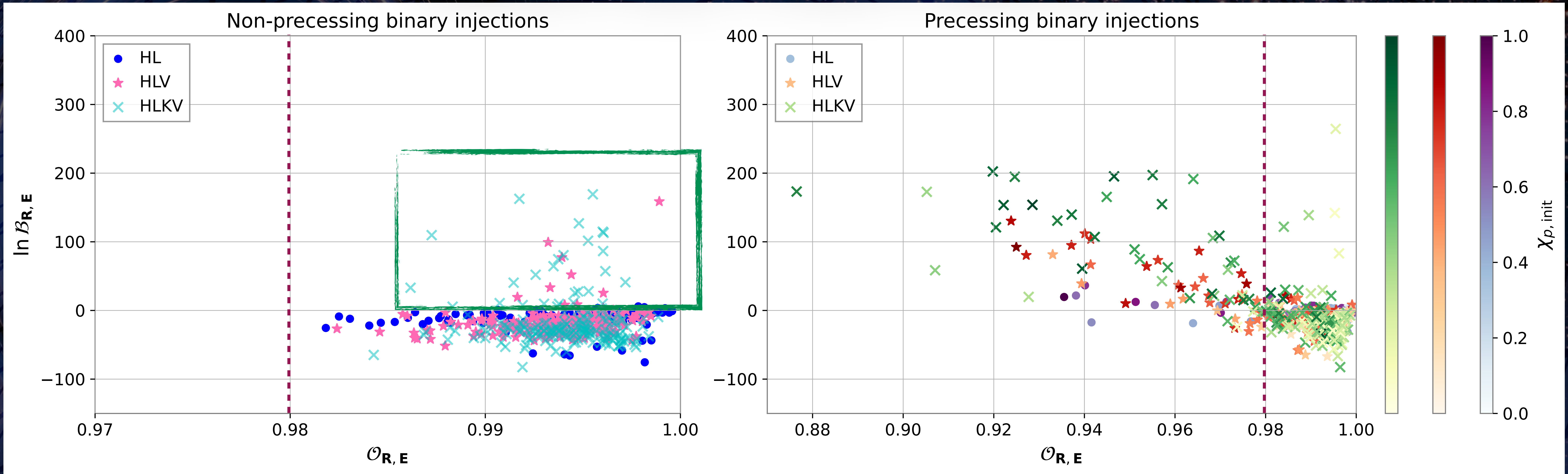

- Events with $\mathcal{O}_{\mathbf{R,E}} \sim 1$ and $\ln \mathscr{B}_{\mathbf{R,E}} \geq 0$ are purely obtained by chance
- We get a very different $\ln \mathscr{B}_{\mathbf{R,E}}$ with different (Markov) chain RNG seeds
- If $\mathcal{O}_{\mathbf{R,E}} \gtrsim 0.98$, $\ln \mathscr{B}_{\mathbf{R,E}} \geq 0$ does not conclusively imply a preference of $\mathbf{R}$ over $\mathbf{E}$

X

(PRELIMINARY RESULTS)

EVENTS WITH $\ln \mathscr{B}_{\mathrm{R,E}} \geq 0$ FOR NON-PRECESSING BINARIES
WHAT DO THEY IMPLY?

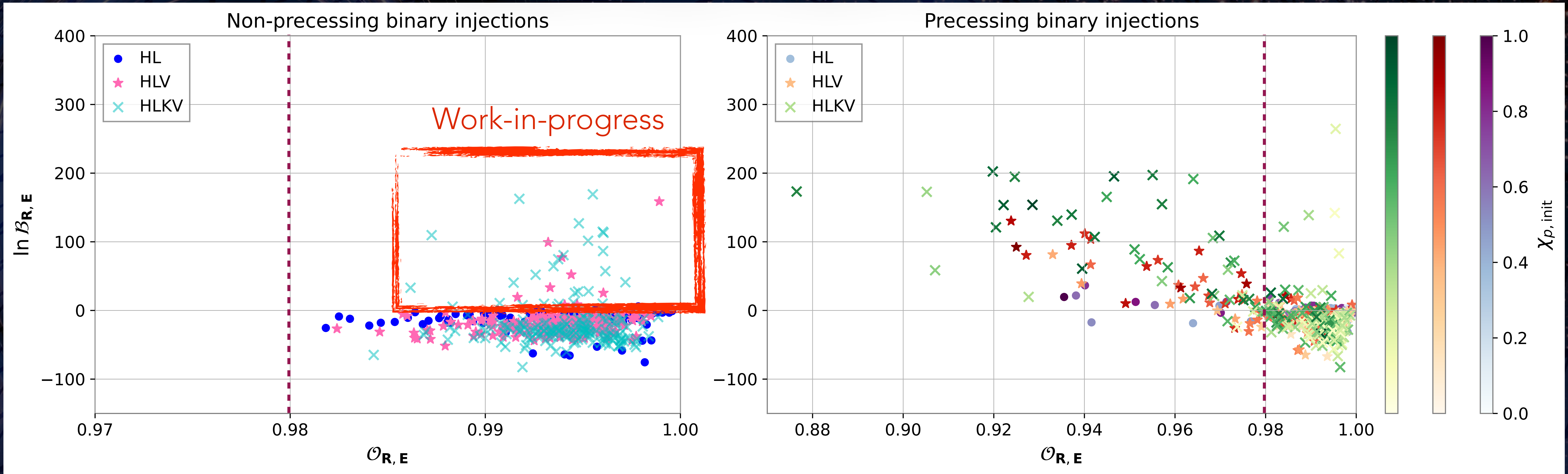

- Under investigation
- Testing stability of evidence computation for relaxed polarization model

SO….
HOW WELL DO THE **E** AND **R** POLARIZATION MODELS REPRESENT GW SIGNALS FROM NON-PRECESSING AND PRECESSING BINARIES?

- Non-precessing binaries are equally well-represented by both **E** and **R**, so if we had to choose one…
  Occams Razor says to pick the simpler one (**E**)
- Precessing binaries with high in-plane spin are generally better represented by **R**

WITH THE RELAXED POLARIZATION (ℝ) MODEL

HOW ACCURATELY CAN *BAYESWAVE* RECOVER POLARIZATION CONTENT OF BURST SIGNALS?

EXTRACTING POLARISATION CONTENT WITH STOKES PARAMETERS (IN LINEAR BASIS)

$$I = |\tilde{h}_+|^2 + |\tilde{h}_\times|^2$$

$$Q = |\tilde{h}_+|^2 - |\tilde{h}_\times|^2$$

$$U = \tilde{h}_+\tilde{h}_\times^* + \tilde{h}_\times\tilde{h}_+^*$$

$$V = i(\tilde{h}_+\tilde{h}_\times^* - \tilde{h}_\times\tilde{h}_+^*)$$

I → Total intensity

Q, U → Linear polarisation

V → Circular polarisation

EXTRACTING POLARISATION CONTENT WITH STOKES PARAMETERS (IN CIRCULAR BASIS)

$$I = |\tilde{h}_R|^2 + |\tilde{h}_L|^2$$

Total intensity

$$Q = \tilde{h}_R\tilde{h}_L^* + \tilde{h}_L\tilde{h}_R^*$$

$$U = i(\tilde{h}_R\tilde{h}_L^* - \tilde{h}_L\tilde{h}_R^*)$$

Linear polarisation

$$V = |\tilde{h}_R|^2 - |\tilde{h}_L|^2$$

Circular polarisation

$$\tilde{h}_R = \frac{1}{\sqrt{2}}\left(\tilde{h}_+ - i\tilde{h}_\times\right) \qquad \tilde{h}_L = \frac{1}{\sqrt{2}}\left(\tilde{h}_+ + i\tilde{h}_\times\right)$$

X

FRACTIONAL POLARISATION

Linear fraction

$$\mathbf{L} = \frac{\sqrt{Q^2 + U^2}}{I}$$

Circular fraction

$$\mathbf{C} = \frac{V}{I}$$

Degree of polarization

$$\mathbf{T} = \frac{\sqrt{Q^2 + U^2 + V^2}}{I}$$

GWs are polychromatic!

All $\mathbf{L}$, $\mathbf{C}$, $\mathbf{T}$ are functions of frequency

and $\mathbf{T} \leq 1$

Born and Wolf, Principle of Optics (1959)

RECOVERING FRACTIONAL POLARISATION

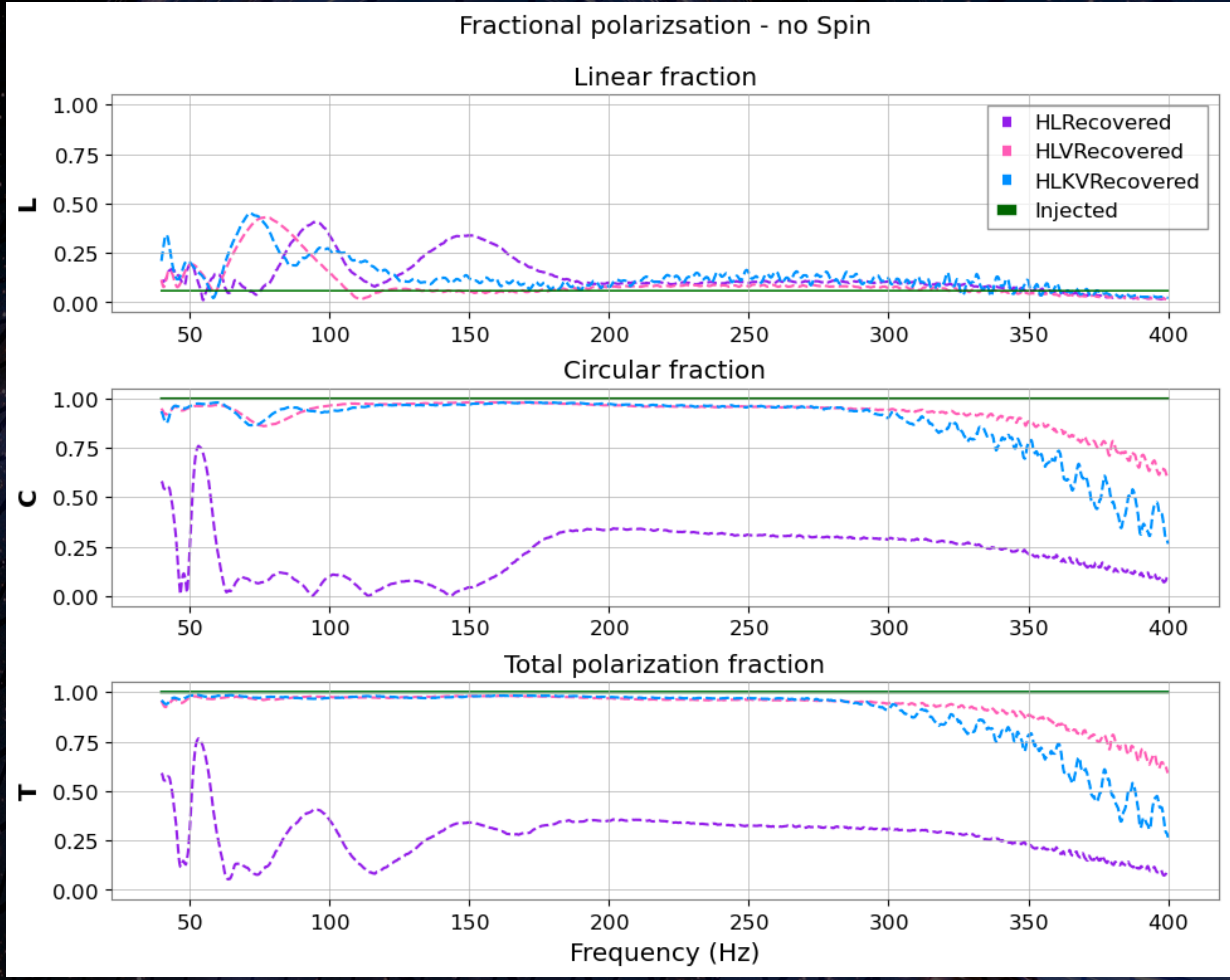

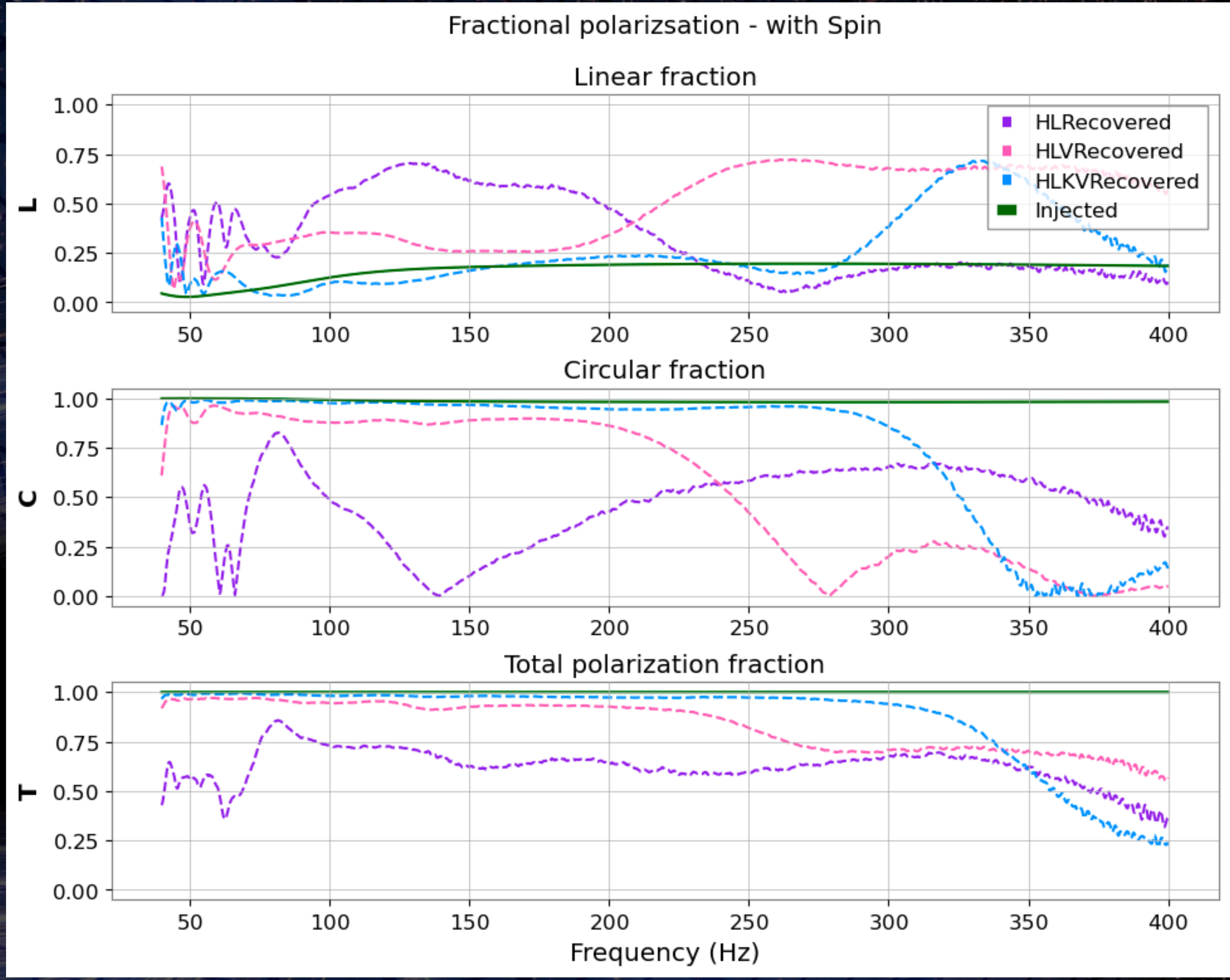

QUANTIFYING ACCURACY OF RECOVERY: SUM OF SQUARED ERRORS (SSE)

Using $\mathbf{L}$ as an example:

$$SSE = \sum_{f_i=f_{\mathrm{low}}}^{f_{\mathrm{high}}} \left[\mathbf{L}_{\mathrm{inj}}(f_i) - \mathbf{L}_{\mathrm{rec}}(f_i) \right]^2$$

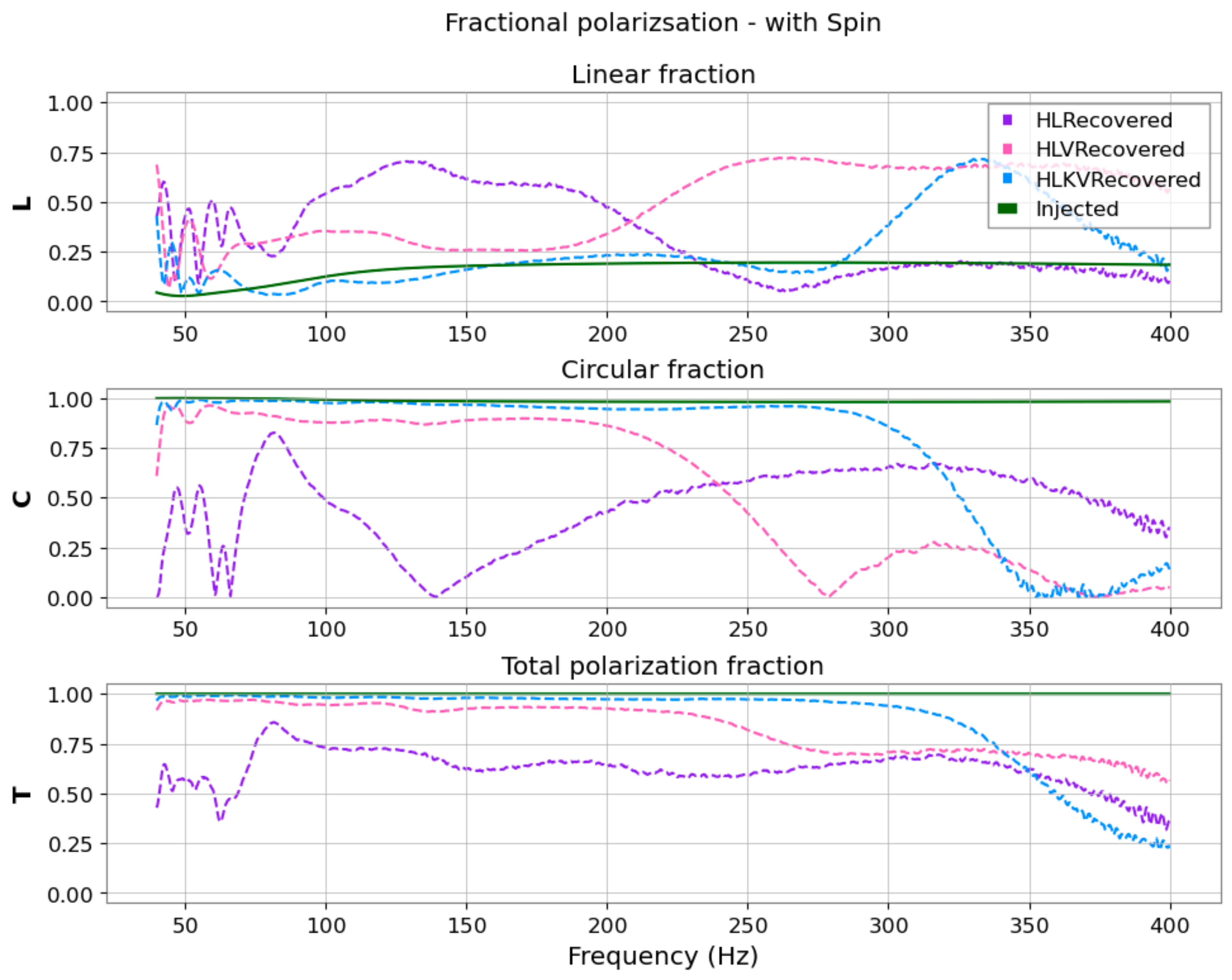

COMPARING RECOVERY FOR DIFFERENT DETECTOR CONFIGURATIONS

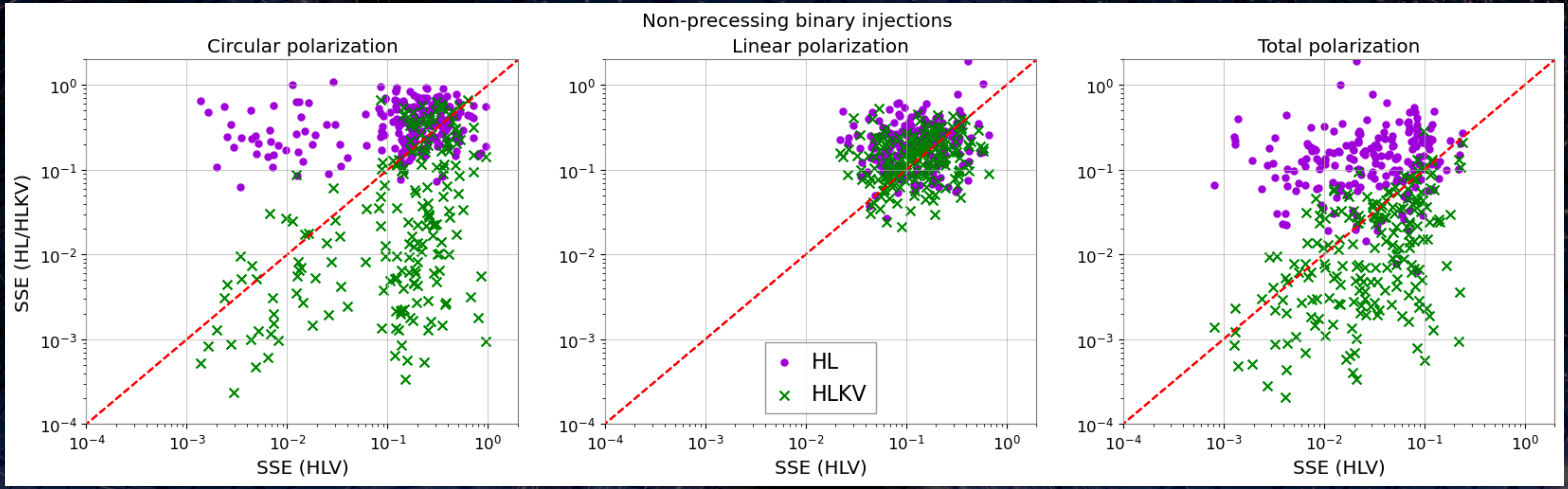

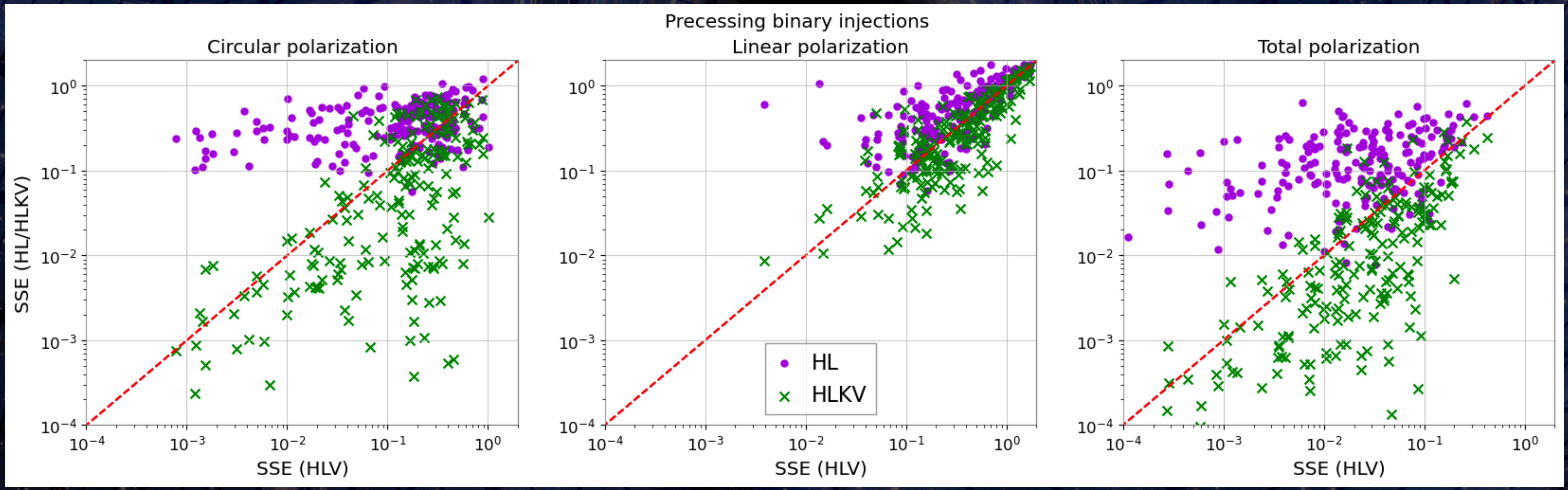

SUMMARY

- Assess *BayesWave*'s ability to characterize GW burst polarizations using simulated precessing and non-precessing BBH signals.
- Compare $\ln \mathscr{B}_{\mathbf{R},\mathbf{E}}$ for the two types of BBH and find increasing evidence for $\mathbf{R}$ with the precessing BBHs, especially when the overlap of $\mathbf{R}$ and $\mathbf{E}$ reduces. Increasing evidence is especially prominent with larger detector networks.
- Larger networks recover fractional polarizations more accurately, using SSE as the metric.
- FUTURE WORK: Expand to more generic transient signals

KEY TAKEAWAY

As the global detector network continues to expand, there is a promising outlook for *BayesWave* in:

(i) more accurately reconstruct precessing and non-precessing binaries with the **R** and **E** models respectively

(ii) more accurately probing the polarization content of GW bursts